Demand-side flexibility in a residential district: What are the main sources of uncertainty?

S. Martinez, M. Vellei, Jérôme Le Dréau

Demand-side flexibility in a residential district: what are the main sources of uncertainty?

S. Martinez[1], M. Vellei[1], J. Le Dréau[1]

[1] LaSIE UMR CNRS 7356, La Rochelle University, France

Abstract

With the increasing share of intermittent renewable energy sources in the energy mix, demand-side flexibility is likely to play a key role in the future. For buildings, flexibility is defined as the ability to shift their energy consumption away from "peak periods" *i.e.* high-demand periods of the electrical network. In France, these episodes occur mainly during the wintertime due to the significant demand for space heating. To achieve flexibility objectives, we explore an indirect control strategy at district scale by adjusting the dwelling thermostat during peak periods. The study is conducted on 337 dwellings in order to better predict the load curve by taking advantage of the aggregation effect. Three main research questions are addressed in relation to the assessment of flexibility potential: (i) the effect of aggregation, (ii) the identification of the most influencing factors, including occupant behavior, and (iii) the quantification of uncertainties. Using an urban building energy modeling tool populated with various national data sources (building envelope, energy class of equipment, etc), we perform a sensitivity analysis on 22 parameters representing the geometry, the appliances, the building characteristics, the occupants, and the grid. The output indicator is the average power shifted during the flexibility (or demand response) event. From this analysis, 7 parameters appear as being the most influential. A regression analysis on these parameters is performed, depending on both the duration of the event and the typology of the district. The results show that the duration of the flexibility event and the occupant pre-selected temperature change are the most influential parameters. It results to approximately ±90 W of uncertainty on an average potential of 290 W of shiftable power per household in a recent district. Furthermore, the occupants are highlighted as making a significant contribution to flexibility. Finally, we observed that the thermal properties investigated with the study of an old fabric district play a key role. Low thermal performance means high heating consumption and increased flexibility potential, but a similar relative uncertainty.

Keywords: urban building energy modeling, bottom-up, district, space heating, demand-response, sensitivity analysis, occupant behavior, probabilistic district characterization

1 Introduction

1.1 Research background

Global warming, fuel poverty, and sustainable development are leading to a growing interest in renewable energy sources, which are often highly intermittent (e.g. solar, wind). As a result, the power grid becomes less robust. In this context, the grid flexibility is defined as the capability of the power system to maintain a balance between generation and load. If the production becomes more intermittent because of an increased share of renewable sources, load adaptation (flexibility) or storage solutions need to be deployed. Consequently, there is an active research field into energy flexibility of the demand. In 2015 Lund *et al.* [1] have published a review of the energy system flexibility measures and point out that the use of dedicated flexibility products such as smart thermostats will become more important with the integration of renewable energies.

The building is an interesting lever to increase the flexibility of the grid as it represents about 30%-40% of the global energy consumption [2]. Indeed, the electricity share of the world residential energy consumption is expected to reach 43 % by 2040 (39% in 2012). Moreover, by 2025, electricity is expected to overtake natural gas as the leading source of delivered residential energy [3] and space heating is seen as a promising source of flexibility. The main challenge of using the flexibility of residential buildings is the small amount of power involved (a few hundred watts) and their controllability. Indeed, the availability of these flexible loads depends strongly on the preferences and activities of occupants. For an individual building, it is therefore challenging to predict the flexibility potential. At the district level, the diversity of uses allows a more reliable response and an increased thermal storage capacity [4]. In addition, for the residential sector, other challenges such as data scarcity and variability in the envelope properties exist.

The IEA EBC Annexes 67 and 82 are dedicated to energy flexibility of buildings [5] and document the growing interest in this topic. Several factors have been identified as influencing flexibility in the literature [6], but they are usually evaluated for individual buildings. Putting forward the key role of aggregation, Hu and Xiao [7] recently proposed a quantification of the flexibility at the district scale with a focus on the role of aggregation.

1.2 Research gaps

When activating energy flexibility in buildings, the aggregation effect has proven to reduce the uncertainty of the predicted power load. As highlighted by Dickert and Schegner [8] for residential applications, electric loads are deeply stochastics. The aggregation effect at the district scale makes the electric load less stochastic than that of a single building, and therefore easier to predict. De Jaeger *et al.* [9] observed a reduction from 65 % down to 10 % uncertainty in the average district energy demand when evaluating a single building compared to 50 buildings. The positive effect of aggregation has also been observed experimentally [10]. With more than 20 apartments, the prediction of the space heating needs becomes less stochastic. Therefore, the energy flexibility of buildings becomes interesting at the district scale so that the Transmission System Operator (TSO) can use this potential.

To evaluate energy flexibility at district scale, an urban building energy model (UBEM) is required. Different models are available [11–14], most of them being bottom-up physical models. The main differences between these tools are the thermal models used (thermal zoning and discretization) as well as the definition of the input parameters, as pointed out by De Jaeger *et al.* [15]. Indeed, UBEM require the adjustment of many parameters, which can be poorly known and stochastic. These parameters are related to the building properties (geometry, envelope, systems) and to the occupants (activities, user-related equipment). Therefore, the correct characterization of these input parameters and their diversity is a challenge. Probabilistic characterization can be used for this purpose [19]. Moreover, there is lack of validation of these tools, especially in the ability to simulate energy flexibility at small, aggregated level (≈100-500 dwellings).

To assess the robustness of the results obtained from UBEM, the quantification of uncertainties is necessary. This can be done with a sensitivity analysis (SA). Among the sensitivity analysis techniques, the Morris method has proven its reliability and effectiveness in the building sector. A detailed presentation of the Morris SA method for optical application is given in [16]. In building applications at district scale, De Jaeger *et al.* [9] evaluated the influence of envelope losses on district energy demand. The average nighttime set point temperature was the main occupant-related parameter influencing the district energy demand. For a single residential building, Vivan *et al.* [17] observed that the level of insulation in summer and the time of the demand response (DR) event in winter were the most influential parameters.

The accurate estimation of the potential can increase the stakeholders participation in energy flexibility [18]. To correctly estimate the flexibility potential at district scale, it is necessary to identify and quantify the uncertainties arising from both building and occupant parameters. In this context, it is particularly important to model the influence of occupants, as they can greatly alter the flexibility potential. In other words, a sensitivity study highlights the main drivers of flexibility at district scale and can be useful in performing a flexibility audit. However, this has not yet been done to the best of our knowledge, due to the challenging aspects of modelling the stochastic behavior of the occupants.

1.3 Research objectives

This paper proposes a methodology to evaluate the uncertainty on the shiftable heating load when activating a group of buildings using heat pump systems. Facing these challenges, a probabilistic characterization methodology with a district database is proposed in this study. Different set point changes (duration and intensity) will be sent to the dwellings, in which the energy use for space heating will be modulated according to the constraints and flexibility tolerances of the users. The stochastic thermostat adjustment behavior of the occupants will be modelled with an agent-based approach. The influence of the input parameters on the flexibility potential will then be evaluated. The results of this study can be used for different purposes: quantifying the uncertainties for control, listing input parameters for a flexibility audit, evaluating the optimal scale of aggregation, providing guidelines on signal design to increase reliability, etc.

To illustrate this methodology, the case study of the Atlantech district (La Rochelle, France) is considered with two levels of building performance (part 2). From this district, an urban building energy model (DIMOSIM) is used to simulate the consumption of buildings (part 3). Finally, a SA using the Morris method and a regression analysis are presented (part 4 and 5).

2 Case study

2.1 District characteristics

The district studied is located in the north of La Rochelle city (latitude 46°2’ North, longitude 1°1’ West, France) in a temperate oceanic climate. The city is mainly composed of low-rise residential multi-storey buildings. The district is composed of 98 buildings divided into 337 dwellings. The weather data file corresponds to the year 2017, classified as typical for future weather conditions, which represent 1904 heating degree days (base 21 °C). This district is mainly composed of couples (with or without children). The dwelling floor area varies from 45 up to 110 m², with an average size of 65 m².

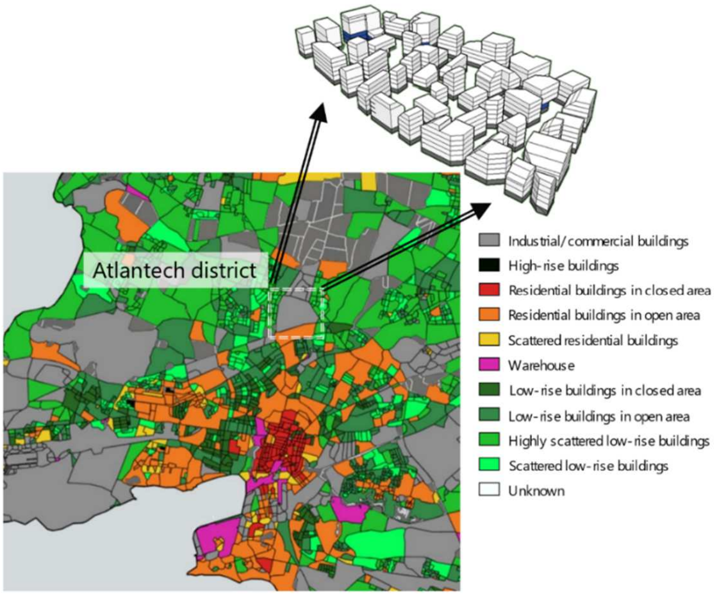

Figure 1: Atlantech district case study. Urbanization database comes from [20]

Two levels of building performance are considered in this study to assess the influence of the construction period on energy flexibility:

- the **new district** (mean consumption for heating of 12 kWh/m².year): the envelope and system properties are defined in accordance with the current French building regulation (2012). Space heating is provided by heat pumps and water-based radiators;
- the **old fabric district** (mean consumption for heating of 100 kWh/m².year): the building properties are defined according to the typical characteristics of multi-storey residential buildings from the period 1982-1989, including renovations. Space heating is provided by direct electric convectors.

In both cases, national databases are used to define the buildings properties (see Annex).

2.2 Flexibility signal

Flexibility is activated every day over the same period, by an economic incentive such as a time-of-use tariff. This strategy was selected as it is relatively inexpensive to implement with smart meters or centralized thermostats. Moreover, it ensures the privacy of the occupants. The French TSO (2017) provides the peak hour distribution. Peak hours mainly occur in the late afternoon (Figure 2), when everybody gets back home. Based on this observation, a price signal is built with a starting time set to 6 pm and a duration from 0.5 up to 3 hours.

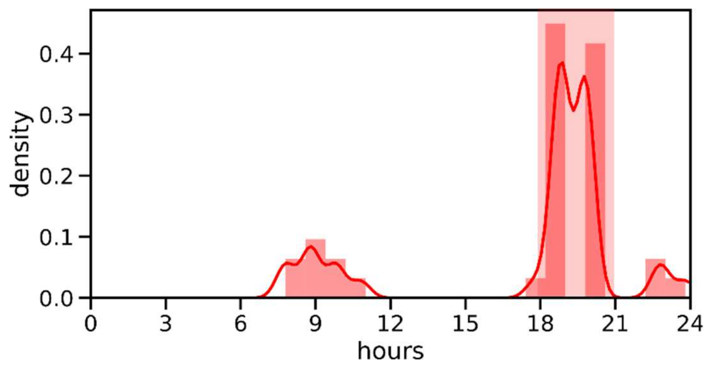

Figure 2 : Daily repartition of the 39 peak hours recorded in France for January 2017; the DR event period considered in this study is highlighted in red

2.3 Flexibility activation in buildings

Once the flexibility signal is sent to the buildings, it needs to be interpreted at the equipment level. To model this flexibility, we based our approach on existing technologies, such as smart thermostats with DR applications [21,22]. The main advantage of this technology is that little extra investment is required, and it ensures the privacy and controllability by users.

The flexibility on space heating is activated semi-automatically by the thermostat of the dwelling, according to the preferences of the occupants (*i.e.* the pre-set tolerated temperature decrease, ΔT). When activated for flexibility, the dwelling set point decreases during the peak period, even if it is unoccupied (Figure 3). In addition, the occupants can interact with the DR signal using the thermostat and modify the set point according to their thermal comfort, which will be discussed in more detail (Section 3.3.2).

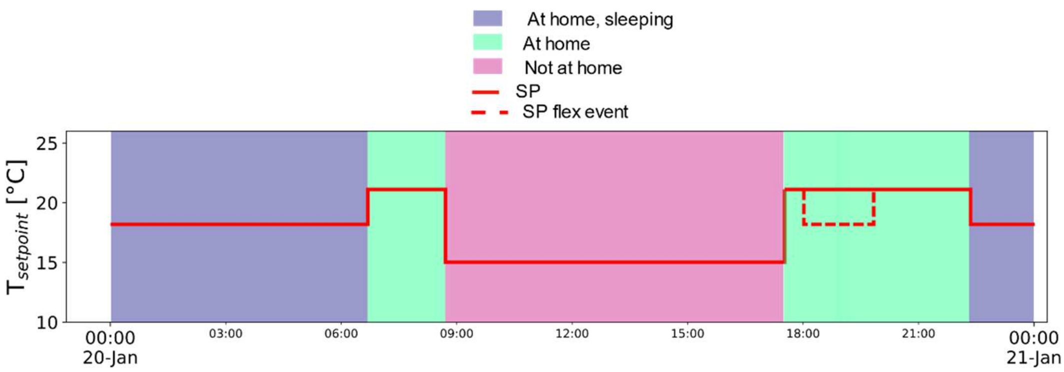

Figure 3: Example of temperature set point in a dwelling (comfort set point of 21°C, setback activated at night and for when not at home and tolerance towards flexibility set at -2°C)

3 Modeling energy flexibility at district scale

The UBEM tool is developed using a bottom-up approach to simulate the thermal and electric load of the residential district. The simulation platform used is a Python-based model (DIMOSIM) developed by CSTB [23–25]. In order to optimize the computation time while affecting the calculation accuracy as little as possible, the recommendations proposed by Frayssinet [26] were followed such as a detailed envelope description to model the heat conduction in walls, a model for the internal mass in order to consider internal inertia of dwellings, a detailed calculation of solar masks to estimate solar gains. The simulation time-step is set to 10 minutes.

Figure 4 provides an overview of the model. The UBEM tools require usually a large amount of information [27], more than 15 000 inputs were filled in for this study. Among the different databases listed (in blue on Figure 4) a selection is made according to the case study in order to obtain a representative dataset. From this selection, preprocessing is performed to convert the data into usable inputs for building energy models, some of them being represented in Figure 5. When possible, these inputs are added to the UBEM as normal distributions, where the mean (μ) and standard deviation (σ) are computed from databases (see Annex). In general, normal distributions appeared as being well representative of the inputs variability observed in the database. For distributions that do not follow a normal distribution, see for example the number of occupants in each dwelling in Figure 5b, a random selection of inputs is performed. In Figure 5, the bins represents the discrete sampling of the distributions, while the lines represent the kernel density estimate of the distribution [28].

The geometry of the district is taken from the land register and the glazing ratio is set according to the orientation of the dwelling. The weather file is used to compute the solar gains and represents the boundary conditions for the heat transfer model. The occupant's characteristics, professional categories, and occupancy rates are given as input to the UBEM. Finally, the usage habits of the appliances, which influence the electrical load and the internal gains are defined for each dwelling. A random process generates diversity in the set of input variables.

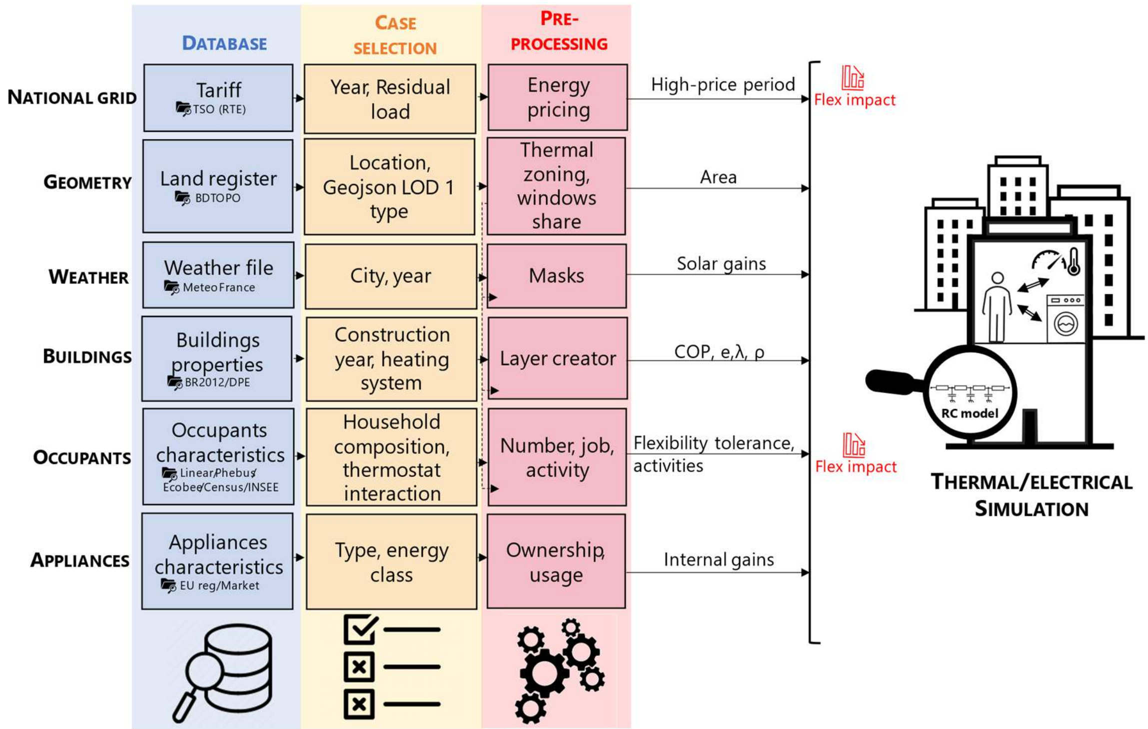

Figure 4 : Overview of the modelling process

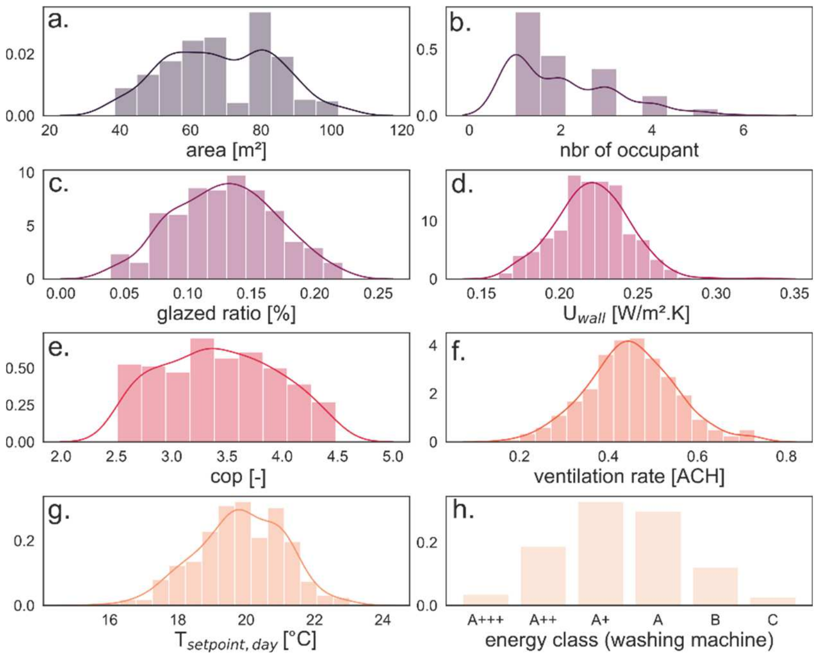

Figure 5: Examples of input distributions for the new district model for floor area (a), number of occupants (b), glazed area ratio (c), wall heat loss coefficient (d), heat pump coefficient of performance (e), ventilation air change rate (f), set point temperature (g) and energy class of systems (h)

3.1 Geometry

The footprint and height of buildings are defined with a land register at LOD1 level of detail. Then, the buildings are split into dwellings assuming a floor height of three meters. Each dwelling is modeled as a single thermal zone, which is acceptable due to the small temperature differences expected between the different rooms [29]. Indeed, the dwellings are characterized by a small volume, a single set point temperature and an inter-zonal ventilation flow rate. The geometry of the district is also used to evaluate solar heat gains, taking into account shading between buildings and openings.

3.2 Buildings

For each building, the composition of the exterior and interior walls, the windows, the floor, and the roof is defined according to the current building regulation [30] or the energy audit database [31]. The databases are analyzed in order to obtain a mean value (μ) and a standard deviation (σ) for the distribution of each parameter.

Space heating is provided by air/water heat pumps for the new district and by electric convectors for the old fabric district. Air-to-water heat pumps are variable speed. The coefficient of performance (COP) of the heat pumps is based on a polynomial regression from the nominal COP to estimate the thermal power output as a function of the temperature difference between the sink (*i.e.* the building) and the source (*i.e.* ambient air temperature). Such a technique, illustrated in [32], has been adapted in the model. The sizing of the heating systems is carried out with an oversizing coefficient of 20 % and the supply water temperature is set to 45°C for the heat pump systems.

Ventilation and infiltration are set according to measurements performed in French households [33]. It is assumed that the dwellings are equipped with mechanical ventilation, humidity-controlled in the case of the new district and constant for the old fabric district. Infiltration is modeled as a constant airflow system, based on n_{50} measurements.

3.3 Occupants

This section describes the main elements of the occupant model: household composition and professional category (3.3.1), occupant activity and presence (3.3.2) and household set point schedule (3.3.3). These models have been introduced, validated, and used in our previous works [34–36].

3.3.1 Household composition and professional category

We first assign a composition to each dwelling by sampling with replacement from the conditional distribution of the household composition conditioned on the usable floor area of the dwelling. These conditional distributions are derived using the summary tables from the INSEE 2015 population census data [37]. The original INSEE household composition categories are simplified using 11 main categories (single adult living alone, single adult with (1,2,3,4) children, couple without children, couple with (1,2,3,4) children, other type).

The professional category (employed, unemployed, student or retired) based on the household reference person is assigned by sampling with replacement from the conditional distribution of the professional category conditioned on the household composition. The status of any other member of the household is assigned based on additional summary tables dedicated to families. Children are assumed to be students.

3.3.2 Occupant activity and presence

To model occupants' activity and presence, we retain the activity sequences or activity profiles available from the French Time Use Survey (TUS) data (2009-2010 TUS campaign) [38]. About 27,900 daily logbooks are used to build the model. These daily times series are clustered according to the professional category of occupants (employee, retired, student, etc) and the type of day (weekend vs. weekday). These two parameters have been selected out of eight independent descriptors as they were identified as influencing the most the activities of occupants [34]. Based on the assumption that most human behaviors are characterized by daily routines, a hierarchical agglomerate clustering is performed within each group to find clusters of similar daily profiles. This clustering used the Jaccard distance as metric and Ward's linkage criterion to group similar schedules, while the number of clusters was identified through the elbow method.

To implement the occupants' activity time series in the UBEM, a stochastic procedure is applied to create different yearly activity patterns by randomly drawing daily schedules within the cluster corresponding to the professional category of occupant and type of day simulated. The outputs of this model are the activities and presence for each occupant of the household. Compared to probabilistic approaches, this method directly uses actual TUS activity sequences and, therefore, allows accounting for the diversity of the real population in terms of occupancy and domestic activities [39].

The activity time series are then converted into time series of metabolic heat rate by using distributions obtained from the ASHRAE reference tables of metabolic rates for common activities [40]. The estimated metabolic heat associated with the occupant's activity is, in turn, an input of the dynamic thermal comfort model. While the status of the occupant (at home, at home sleeping, not at home) is an input of the thermostat adjustment model.

3.3.3 Set point schedule

In our occupant modeling approach, we assume that each household is equipped with a programmable thermostat (see Section 2.3), which can be used to set a schedule for:

- $T_{setpoint,\ day}$: the day set point temperature when somebody who is not sleeping is at home;
- $T_{setpoint,\ night}$: the night set point temperature when everybody who is at home is sleeping;
- $T_{setback}$: the setback temperature when nobody is at home.

For each household, the schedule is estimated based on the occupants' activity and presence profile time series by calculating the hourly probability of having each household's status (at home, at home sleeping, not at home) over the simulated period. For each hour of the day and depending on the activity of the occupant, the status with the highest probability of occurring defines the corresponding hourly scheduled/default temperature for the household. This hourly profile is repeated for each day (Figure 3). Thus, the hourly set point schedule is defined for each household in a pre-process with respect to the dynamic thermal simulation, while the manual thermostat adjustment behavior is dynamically simulated.

Defining an operation schedule does not necessarily imply that each household is using a night set point temperature or a setback temperature. The probability of using either a night set point temperature or a setback temperature is equal to 80 % based on the PHEBUS dataset [41]. The $T_{setpoint,\ day}$ distribution is also based on the PHEBUS dataset (Figure 5). Each occupant adapts its default clothing level based on the $T_{setpoint,\ day}$ in order to obtain a neutral PMV value. The default clothing insulation and the default set point temperature can then be modified by the occupants over the course of the dynamic simulation (see 3.5).

3.4 Appliances

The appliances are randomly allocated to the households based on the appliances' ownership rate conditioned on the household size and the professional category and calculated using aggregated data from the PHEBUS dataset [41]. As the conditional distributions were not available, the capacity and energy class of the appliances cannot be conditioned on the household size and the professional category. The marginal distributions of the capacity of the appliances were available from the ADEME survey campaign [44]. The marginal distributions of the energy class of the appliances were built from the marginal distributions of the age of the appliances combined with sales data [49].

The appliances' electricity load curves are randomly assigned to the activity starting times based on the capacity and the selected energy class of the equipment (ranging from A+++ to C). In total, 1200 load curves are built based on the EU labeling scheme for electronic devices. The electrical load is then converted into internal heat gains according to emission factors. In total, approximately 85 % of the electricity used by appliances is converted into internal heat gains, which is in accordance with [42].

3.5 Modeling flexibility from occupants

Occupant thermostat adjustments can occur because of rejection of DR events, change of metabolic rate, or thermal discomfort due to mismatch between schedule and presence (Figure

6). The thermostat adjustment behavior is modeled using an agent-based approach: each member of the household is represented as an agent with a set of attributes (status, clothing, and metabolic rate) and a set of possible adaptive actions (set point and clothing adjustment). User interaction data from about 9,000 connected Canadian thermostats included in the Donate Your Data (DYD) dataset [43] are used to calibrate the thermostat adjustments model [21].

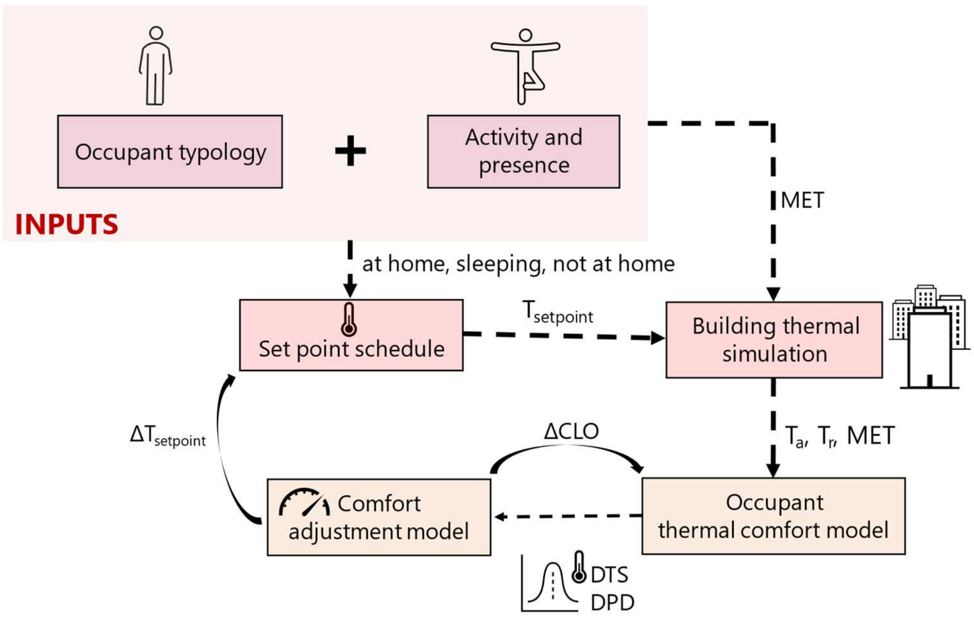

Figure 6 : Overview of the modelling framework for thermostat interactions.

The adaptive principle [44] is assumed to be determining the manual overriding behavior. For modeling the agent's adaptive behavior, we use a particular type of agent: the Belief-Desire-Intention (BDI) agent [45]. In this study, environmental and personal conditions form the agent's thermal dissatisfaction, which is represented by the Dynamic Thermal Sensation (DTS) and Dynamic Percentage of Dissatisfied (DPD). DTS and DPD predictions are based on a thermo-physiological model coupled with a dynamic thermal perception model [35]. This dynamic evaluation of thermal comfort appears necessary given the short timescale associated with demand response events.

Then, the agent translates its thermal dissatisfaction into a desire about what to achieve. This action is predicted using a time-dependent Bernoulli process. A uniformly distributed random number (n) in [0,1[is compared to the DPD. If the DPD is higher than n, the outcome is to change its current state. The agent's intention is defined by the probabilities of adjusting during a 2-min time interval (using a time-dependent Bernoulli process):

1- the clothing $p_{adj,\ clothing}$ (before), with a mean value of 10.5 % and an observed range of 3-18% based on the calibration with the DYD dataset,

2- the set point temperature $p_{adj,\ SP}$ (afterward), with a mean value of 3.5 % and an observed range of 1-6%.

Thus, it is assumed that the adjustment of the clothing insulation is the preferred adaptation strategy.

When the agent decides to adjust its clothing, he does it by either increasing or decreasing the clothing of $\Delta CLO = 0.1$ clo where 0.1 clo is, for example, the clothing insulation change made when passing from a thin long-sleeved sweater to a thick long-sleeved sweater [46]. While, when the occupant decides to adjust the set point of $\Delta T_{setpoint}$, he does it to restore thermal neutrality (*i.e.* towards a PMV ~ 0). The $T_{setpoint}$+ $\Delta T_{setpoint}$ has a lower limit equal to $T_{setpoint,day}$ -1°C during warm exposures and an upper limit equal to $T_{setpoint,day}$ +6°C during cold exposures, based on observations of the DYD dataset.

3.6 Thermal/electrical models

The building thermal model is a detailed physic-based RC model [23]. The elements of the dwelling are discretized into exterior walls, windows (divided per orientation), interior walls, floor, and roof. The opaque walls are discretized in four layers, namely the external finish, the thermal mass, the insulation, and the interior finish, which leads to more than 20 capacities for each thermal zone. The conduction through the walls is then solved by the finite difference method, with a time-step of 10 minutes.

The electrical load of the buildings is calculated from the space heating and the equipment consumption on a 10-minute time-step.

3.7 Qualitative validation of the model

Validating the results of UBEM tools is a challenging task due to the lack of standardized data, the lack of information and the complexity of the tools. Comparison with measured data cannot be performed because only half of the Atlantech district has been built to date. Therefore, the model validation focused on the thermal model, the input parameters, and the simulation results with external references.

The thermal model of the DIMOSIM tool was compared with the results of the benchmark tests BESTEST [47] (free-running and heating cases) and DESTEST [48]. DIMOSIM shows good agreement with the other tools, both in terms of temperature and energy.

Given the large number of input parameters required for the design of the district (around 15 000 for this district), the control of these parameters with typical values is of main importance. The heat loss coefficient (HLC) of each dwelling was compared to ensure the overall performance of the district. Additionally, each energy usage was also checked.

Figure 7a represents the average daily electrical load profiles of the devices within the district. The average daily profile was compared with the results of Vorger [49]. Vorger's results, also based on a bottom-up model, correspond to the mean power of 100 dwellings randomly selected. The differences observed can be partly explained by the better energy classes selected for the electrical appliances, especially for the fridge. Moreover, Vorger's results are focused on a French representative set of buildings that includes single-family houses equipped with more electrical devices than dwellings. The simulated annual electricity consumption of the appliances (27 $kWh/m^2_{heated\ area}.year$) corresponds to the mean value measured in French collective buildings [42]. Additionally, the coincidence factor was assessed to verify the diversity of uses within the district (Figure 7b). This factor is equal to the peak load of a district divided by the sum of the peak loads of its individual buildings. These values are compared to the relationship proposed by Velander (1947) for the energy consumption of appliances with electrical heating. The diversity of uses appears to be consistent within the district, slightly below the values proposed by Velander. Similar observations were made by Sørensen *et al.* [50], in which the measured peak power was about 20% lower than Velander's formula (for 1000 apartments). The resulting heating consumption of the new district is equal to 12

$kWh/m^2_{heated\ area}$.year with a relatively large standard deviation between dwellings. Despite similar thermal properties, not all buildings can benefit from passive solar heat gains within the district.

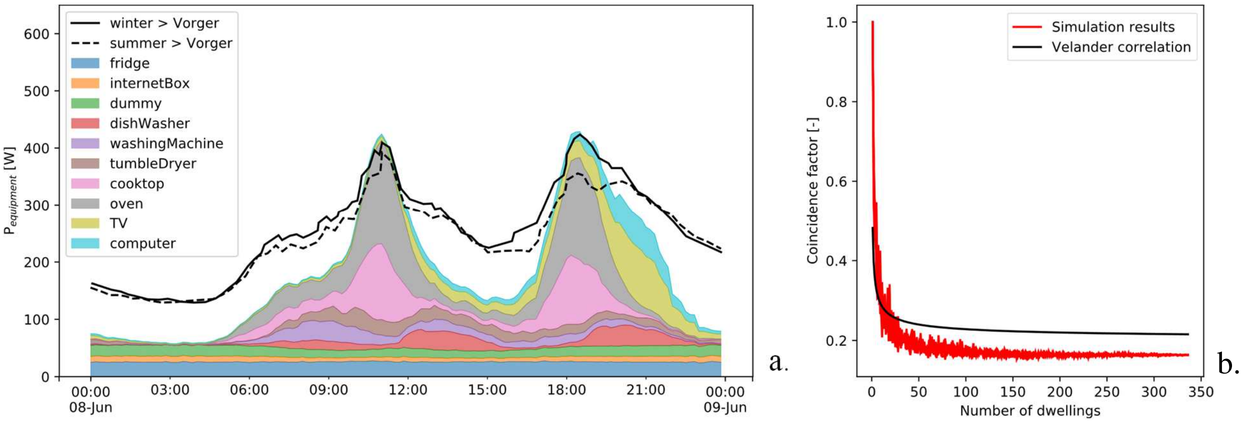

Figure 7: Average electrical load per household from appliances, heating excluded (a) and coincidence factor, heating included (b).

3.8 Examples of load curves

The time series representation of the UBEM output is presented (Figure 8) for the district and for three cold days of the winter (20^{th} to 23^{rd} of January). The DR event occurs between 6 and 9 PM, during which the set point is lowered in each dwelling with a different amplitude. The results presented are the average values of operative temperature and heat-pump electrical load for the district. The upper graph presents the average set point, the 0.95 and 0.05 quantile of the operative temperature distribution and the average operative temperature of the dwellings, while the lower graph represents the average electrical load of the heat pumps.

During the day, there is a significant gap (about 2 °C) between the average operating temperature and the set point. This can be explained by the fact that the set point is reduced during unoccupied periods (15 °C of set point when dwellings are unoccupied), while inertia and solar gains have the effect of maintaining the operative temperature. During the flexibility event, the thermal inertia of the housing explains the gap between the set point temperature and the operative temperature.

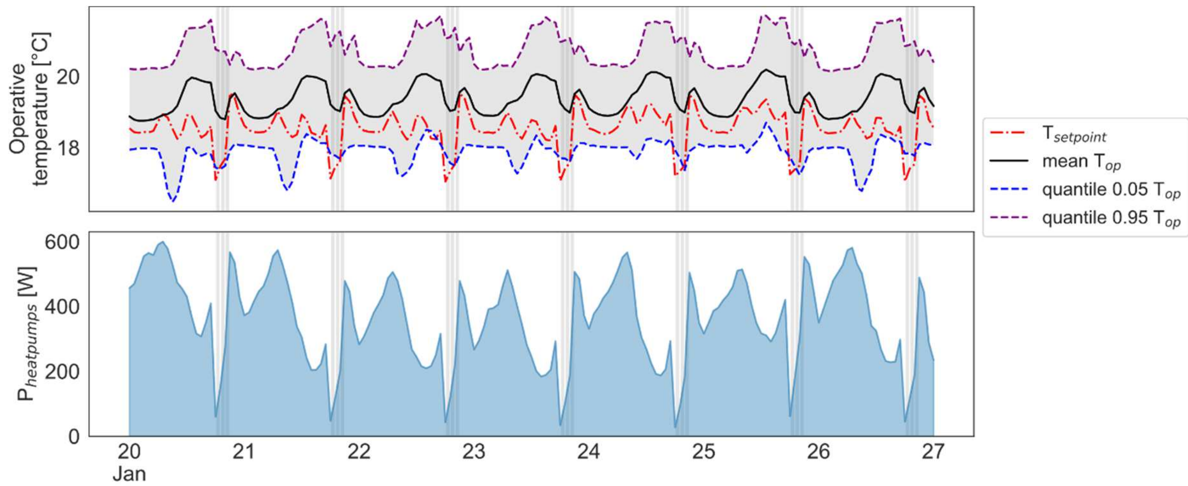

Figure 8: Overview of the time series collected as the output of the UBEM during 3 days of January

4 Methods

4.1 Indicator to characterize flexibility

The most common indicators found in the literature to characterize the flexibility are the amount of power change, duration of the change, rate of change, response time, shifted load and maximal hours of load advance [1,51,52]. Based on the previous works, we have decided to consider the mean power shifted away from a peak period to assess flexibility at the district scale. Since most peak hours occurs during the winter, we decided to focus on January, which was the coldest month of the year 2017. The average shifted power during a peak period is given by:

$$P_{\text{shifted}} = \sum_{\text{peak hours}} \sum_{\text{dw}} \frac{P_{\text{ref,dw}}(t) - P_{\text{flex,dw}}(t)}{N_{\text{dw}} \cdot N_{\text{peak hours}}} \tag{2}$$

Where $P_{ref,\,dw}$ is the heat pump electric load (in W) during peak hours for the reference case, i.e. without DR event, $P_{flex,\,dw}$ the heat pump electric load (in W) during the DR event, $N_{peak,\,hours}$ the number of peak hours during January and N_{dw} the number of dwellings (dw).

To illustrate the calculation of the indicator, we show the evolution of the district-averaged heat pumps power for both reference and flexibility cases (Figure 9). The simulation focuses on the average electrical power of air-to-water heat pumps in the 337 dwellings of the district. The long-lasting rebound effect can be observed. It is useful to recall that, in our model, the occupants adjust the set point temperature during peak hours in case of thermal discomfort.

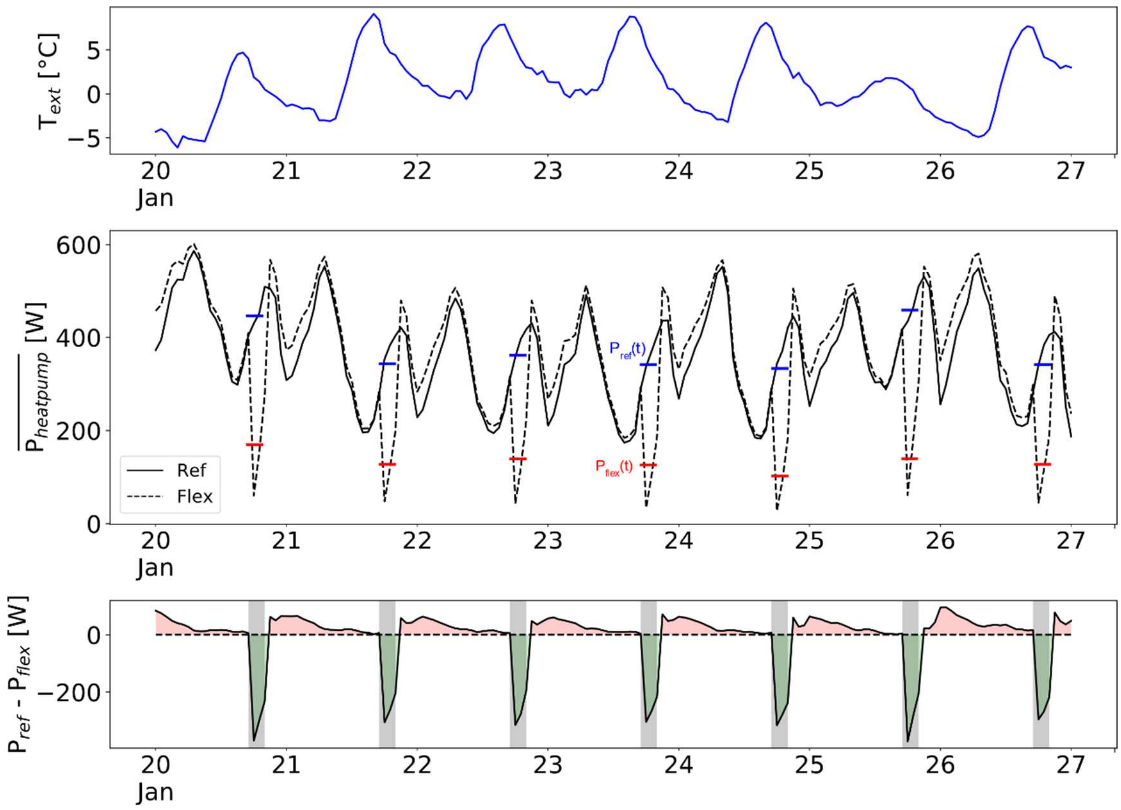

Figure 9 : Example of a response of the mean electrical power of the heat pumps, new district case-study

The aggregation effect on the electrical load prediction is highlighted in Figure 10. The indicator was calculated from 1 to 674 dwellings to evaluate the effect of the district diversity (both from buildings and occupants). From Figure 10, we observe that the increase in the number of dwellings reduces the uncertainty in the calculation of the indicator. In green, the average error, defined as the ratio of distance between the maximum and the minimum value of $P_{shifted}$ to the mean $P_{shifted}$ value, is represented. 337 dwellings appear sufficient to obtain a robust calculation (10% error). The uncertainty in the value of $P_{shifted}$, depending on the number of dwellings, follows a Student's t-distribution with a 95 % confidence interval that is representative of a random behavior in the sample. According to the t-student distribution results, a district of 500 dwellings is needed to estimate the $P_{shifted}$ indicator with an error of 5%. Wang et al. [53] found that 700 dwellings were necessary to decrease uncertainty under 10 %. These differences can be explained by several facts: (i) in Wang's study the shiftable power is not averaged over the entire DR event and (ii) the flexibility is only activated during unoccupied hours leading to a reduced number of considered households, (iii) in our study the period of activation of flexibility starts at 6 PM, which is a time when the probability of dwellings being unoccupied is low.

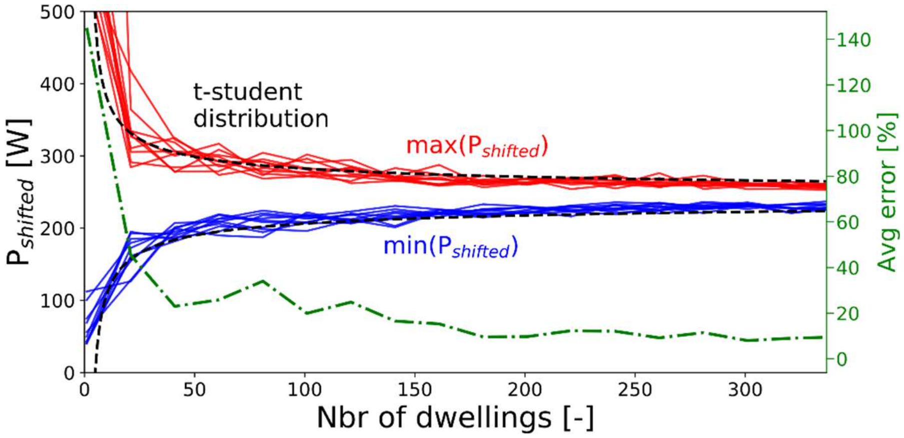

Figure 10: Aggregation effect on the mean shifted power calculation, minimum (blue), maximum (red) values and average error (green)

4.2 Identification of the most influential parameters: the Morris method

The method of Morris [54] consists of segmenting the model inputs within their range of variation. Thus, this segmentation generates a unit hypercube of input variables that will be used in the model to evaluate the change in the output for each parameter variation. The sensitivity measured at each point (elementary effect) can be defined by the ratio between the output and the input displacement. For a user-defined number of trajectories, the Morris method evaluates the mean and the standard deviation of the elementary effect. For this study, the input parameters are assumed to have a uniform distribution. For the 22 selected parameters concerning buildings characteristics, occupant and appliances, the mean values (μ) of the distribution are changed and their impacts on the flexibility potential is assessed. The output considered is the flexibility potential (see 4.1).

This screening method has been widely used and described in the literature [55–57] including for building applications [58]. The method of Morris method appears as a robust and time-efficient method. For these reasons, it was selected for this study.

To process a Morris sensitivity analysis, it is necessary to:

- define a set of relevant parameters;
- determine their range of variation;
- select an indicator that is well suited to the phenomenon under study.

The originality of this sensitivity analysis comes from the fact that the inputs are not deterministic values but normal distributions. Figure 11 provides an overview of the method used.

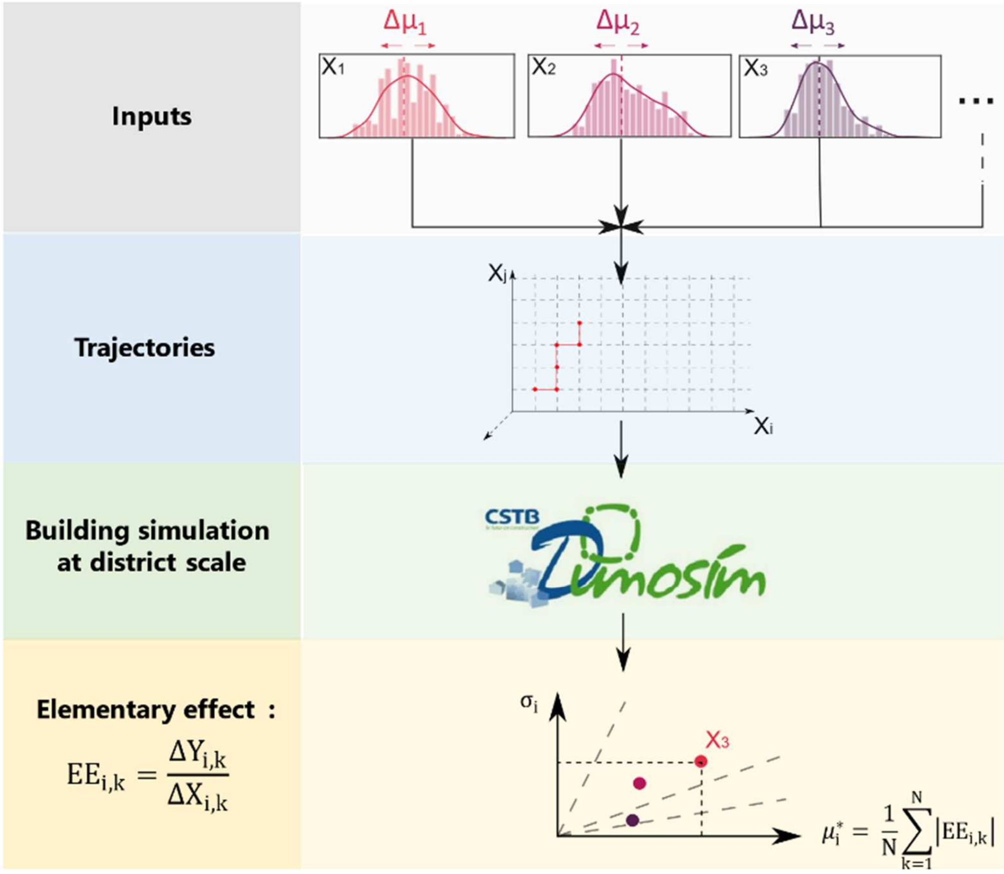

Figure 11 : Overview of the methodology, from input definition to analysis of the results

In Figure 11, EE represents the elementary effect, $\Delta Y_{i,k}$ is the output difference for the *k* parameter at the *i*-th trajectory defined as $f(X_i+\Delta x)-f(X_i)$ where *f* represents the UBEM model, $\Delta X_{i,k}$ is the grid step of parameter k, for the *i*-th trajectory.

To determine the most influential parameters, we conducted a 100-trajectories and 4-grid jump test with the parameters listed in Table 1. The grid jump is the number of samples into which each parameter is divided. The convergence of the results was checked and found to be well suited for the identification of the influential input parameters.

In Table 1, the parameters (i) are well defined and the determination of (μ, σ) was done by database analysis (part 3 and Annex 1). The mean of the input is changed between μ-$\Delta\mu$ and μ+$\Delta\mu$ based on the standard error of the mean ($\Delta\mu=2\times\sigma/\sqrt{n}$, with n=98 buildings). Diversity in the district will be provided by the standard deviation (σ) of the distribution, which remains unchanged. The parameters (ii) are derived from a limited set of data, therefore, for these parameters we have defined a 10 % uncertainty on the mean, or an ad hoc value of this uncertainty. The parameters (iii) are set equally for all the dwellings of the district.

In addition to the parameters presented in Table 1, the influence of the building and occupants' diversity and stochasticity was evaluated. In the UBEM tool, these random processes are characterized by two parameters:

1. the random characteristics parameter ($random_{characteristics}$), which influences the selection of occupant and building properties. It allows the district to be populated with a diversity of occupant and building characteristics;

2. the random occupant behavior ($random_{occupant}$), which influences the sequencing of the occupant behavior model (presence, activities and thermostat adjustments). It allows to simulate the stochasticity of occupant behavior.

Table 1 : Parameters of the sensitivity analysis, mean value, standard deviation, and range of variation ("-" means that no variation among buildings was defined)

	Name	Description	μ	σ	SA bounds [μ-Δμ; μ+Δμ]	unit	
Geometry	glazedRatio	Average glazed ratio of the dwelling	13.5	3	[13, 14]	%	
Buildings	Uwall	Heat loss coefficient of the walls	0.22	0.035	[0.21, 0.23]	W/(m²K)	
	Uwindow	Heat loss coefficient of the windows	1.23	0.16	[1.2, 1.26]	W/(m²K)	
	Ufloor	Heat loss coefficient of the floor	0.2	0.055	[0.19, 0.21]	W/(m²K)	
	Uroof	Heat loss coefficient of the roof	0.13	0.042	[0.12, 0.14]	W/(m²K)	
	Q_{ventil}	Air change rate (ventilation & infiltration)	0.55	0.15	[0.49, 0.61]	vol/h	
	massthickness (iii)	Equivalent thickness of the concrete core to model the inner mass	0.1	-	[0.05, 0.15]	m	
	COP	COP of the air/water heat pump	3.33	0.81	[3.17, 3.49]	-	(i)
Appliances	cooktop	Energy class of the cooktop	5.1	0.8	[4.94, 5.26]	-	
	tumbledryer	Energy class of the tumble dryer	5.15	0.72	[4.98, 5.28]	-	
	dishwasher	Energy class of the dishwasher	3.12	1.13	[2.9, 3.36]	-	
	fridge	Energy class of the fridge	3.52	0.94	[3.33, 3.71]	-	
	oven	Energy class of the oven	5.11	0.8	[4.99, 5.31]	-	
	washingmachine	Energy class of the washing machine	2.75	1.24	[2.51, 2.99]	-	
Occupant	setpoint	Average heating set point (day) of the building	19.83	1.26	[19.58, 20.08]	°C	
	setback	Probability of a dwelling to decrease its set point when unoccupied and sleeping	80	10	[72, 88]	%	
	ΔT	Pre-set set point difference during a flexible event	1.5	0.5	[1, 2]	°C	
	padjSP	Probability for occupant to adjust their set point due to discomfort	3,5	-	[1, 6]	%	(ii)
	padjclothing	Probability for occupant to adjust their clothing due to discomfort	10,5	-	[3, 18]	%	
	presence	Probability of occupancy of the dwellings	100	-	[80, 100]	%	
Grid	durationEvent	Duration of the flexibility event	105	-	[30, 180]	min	(iii)

4.3 A better understanding of the uncertainty of parameters: the regression analysis

For the most influential parameters identified by the SA, another computation is made by modifying "step by step" the parameter, holding other factors constant, and performing a linear regression analysis of the flexibility potential indicator ($P_{shifted}$). The impact of the parameter is quantified using the following three indicators:

- The **mean value** of the $P_{shifted,}$ represents the average value of the flexibility potential for each parameter tested;
- The **range of variation** (Δ) between the maximum and minimum value of the flexibility potential ($P_{shifted}$) gives an idea of the variability of the parameter;
- The **R^2 coefficient** calculation indicates the predictability of the impact of this parameter on the flexibility potential of the district.

5 Results

We first identify the parameters influencing the most the flexibility of the new district (part 5.1). We will later study the performances of a typical old fabric district (part 5.2).

5.1 New district

5.1.1 Morris screening method

Figure 12 presents the results of the sensitivity analysis for the new typical district. The Figures represent the SA-mapping of the parameter and the μ* distribution. Most of the investigated parameters are considered as little dependent on each other because they are below $\sigma/\mu^* = 1$ [54]. Moreover, the limited number of trajectories explain some high values (*i.e.* in the order of magnitude of the mean effect) of the standard deviation of the parameters. However, we consider these results robust enough in order to detect the most influential parameters.

With regard to the random parameters, it appears that a Morris sensitivity analysis is not suitable to explore their influence. Thus, we decided to explore these elements separately in Section 5.1.2.

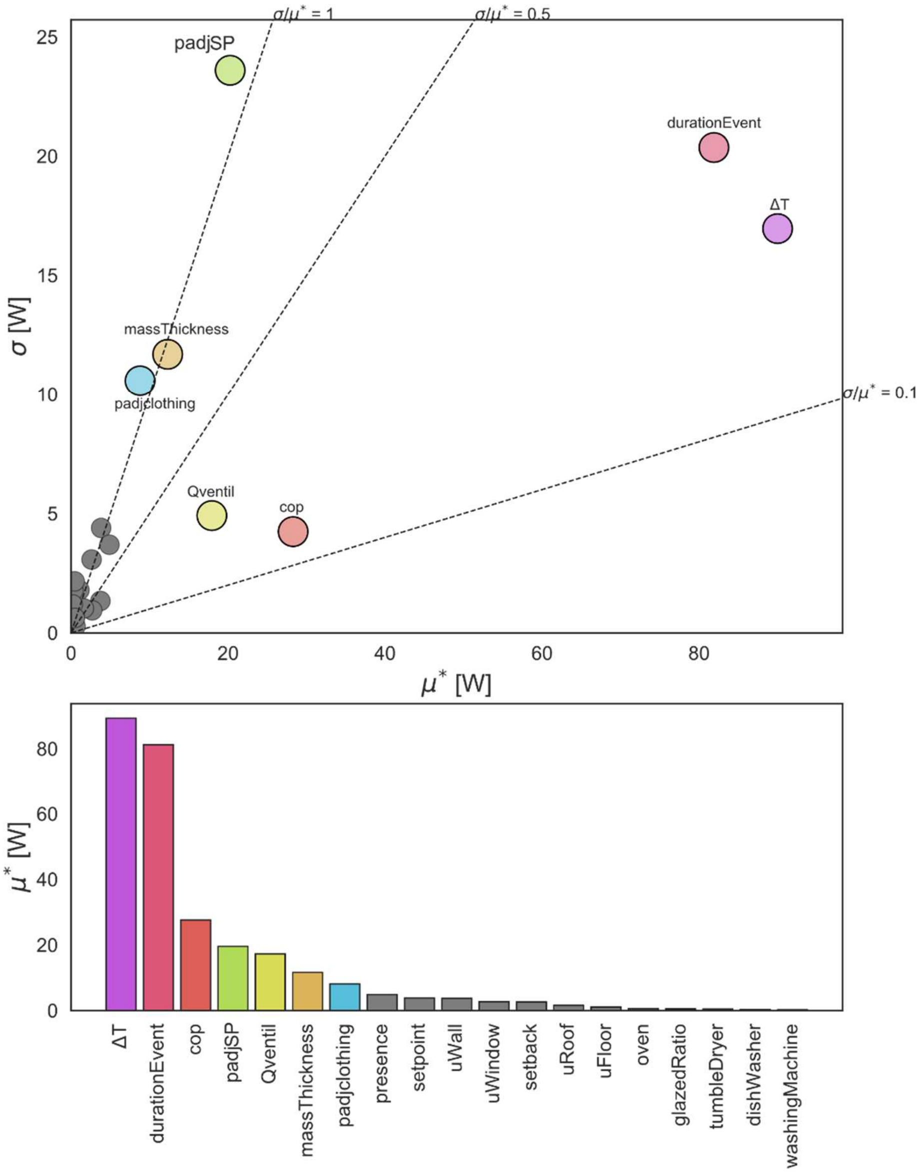

Figure 12: Sensitivity analysis, σ-μ* plot and μ* distribution for the average shifted electrical power of the district during the month of January – $P_{shifted\ avg}$ = 290 W

The average flexibility potential ($P_{shifted}$) was calculated at 290 W. It appears that the duration event (*durationEvent*) and the set point decrease during the flex event (*ΔT*) are the key parameters of the study as its μ* value (80 W) represents approximately 30 % of the average flexibility potential. Therefore, these two parameters need to be known by the aggregator/district manager to evaluate correctly the flexibility potential.

An illustration of the importance of the duration of the event on the flexibility potential is presented below. On Figure 13, the increase in the electrical load after the shutdown of the heat pumps (especially for the long modulation) indicates that some households have reached their lower set point. Moreover, the longer the flexibility event, the more likely the operative temperature in the dwelling will decrease below a comfort temperature, so an adjustment in the set point from occupant will occur to increase the indoor temperature.

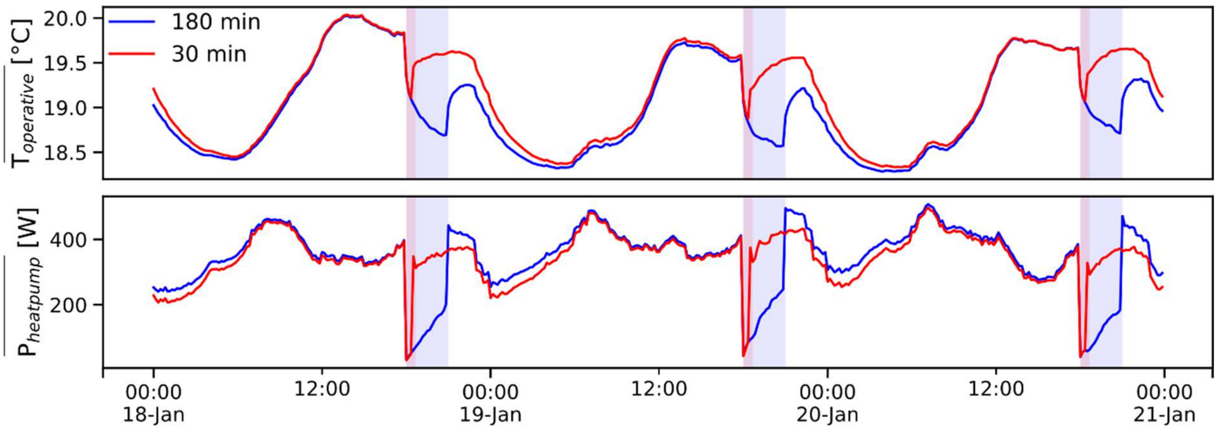

Figure 13 : Effect of the event duration on the average operative temperature and the average heat pump consumption

Thus, we observe that the event duration indicator can modify the influence of other parameters. Figure 14 shows the combined effect of *durationEvent* and *ΔT*. For a short modulation, we detect that $P_{shifted}$ is higher compared to a long modulation as the operative temperature is less likely to reach the lower set point due to thermal inertia. Thus, no matter how low the set point temperature is, the heating system will stop. Consequently, the flexibility potential will be less dependent on the temperature difference (lower slope of the regression line).

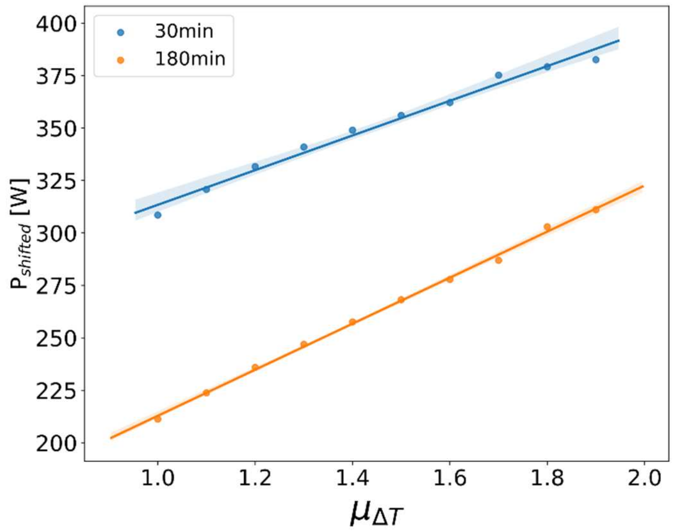

Figure 14 : Influence of the set point decrease and duration of the DR event on the flexibility potential.

The third most influential parameter is the efficiency of the electrical to heat conversion of the heatpump system (*cop*, μ* = 30 W). Then, the probability of thermostat adjustment ($padj_{SP}$) is observed to be influential (μ* = 20 W). The ventilation rate (*Qventil*) plays also an important role in the flexibility potential evaluation as it represents a non-negligible part of the thermal losses in these well-insulated buildings. For similar reasons, the *massThickness* influences the $P_{shifted}$ value as it represents the thermal inertia of the housing partitions. Finally, the probability of clothing adjustment ($padj_{clothing}$) is observed as being important. This parameter, and also $padj_{SP}$, are related to the behavior of the occupants. An increase in the probability of thermostat adjustment leads to an increase in the probability of rejection of the flexibility event, and thus a decrease in the flexibility potential of the neighborhood. Conversely, an increase in the likelihood of thermal comfort adjustment through clothing changes will decrease the number of rejections, and thus increase the flexibility potential. The 7 coloured parameters (Figure 12) were defined as the most important parameters.

The low influence of the *setpoint* in the sensitivity analysis results should be taken with caution. Despite a mean district setpoint relatively well-known at this aggregated scale (±0.25°C), other thermostat-related parameters show an influence on flexibility (e.g. $padj_{SP}$, *presence* and *setback*). Moreover, some combined effects can be observed: a low set point will, for example, change the effect of the ΔT due to a limit in the clothing insulation. Therefore, it is important to remember that the *setpoint* controls the heating consumption and therefore plays an important role in assessing the potential for flexibility.

5.1.2 Uncertainty estimation based on regression analysis

For each of these 7 parameters and the 2 random parameters, the coefficient of determination (R^2), the mean value (mean) and the range of variation (Δ) of the shifted power are presented in Figure 15 (180-minute DR event) and in Figure 16 (30-minute DR event) for the bounds defined in Table 1. In both cases, relatively high values of R^2 parameter are observed for ΔT, *Qventil*, *cop, massThickness*, $padj_{SP}$ and $padj_{clothing}$, demonstrating a correlation between the variation of these parameters and the shifted power.

The results confirm the Morris analysis performed previously. We observe that the potential of flexibility is greater in the case of short-term modulation (+ 90 W approximately). For both tests, the set point decrease is also the main source of uncertainty in the district flexibility (Δ = 100 W for the 180 min DR event, 74 W for the 30 min DR event).

Parameters related to the type of occupant ($padj_{clothing}$, $padj_{SP}$, $random_{charac}$ and $random_{occ}$) and to the system efficiency (*cop*) are found to play a role but to a lesser extent (10-30 W). The efficiency of the system plays a similar role (approximately 20 W of uncertainty) than occupant-related parameters. Finally, the *massThickness* and the *Qventil,* considered as building and envelope related parameter represents about 20 W of uncertainty.

By comparing the results for the two durations of DR events, the interaction of occupants with the thermostat is discussed. For a 30-min DR event, we observe that an increase of $padj_{SP}$ increases the flexibility potential. This result may look unexpected, because this parameter seems to be related to the possibility of rejecting flexibility, so increasing $padj_{SP}$ should reduce the flexibility potential. However, with the increase of $padj_{SP}$, the set temperature of residential area will also increase, especially during cold days. In fact, in cold and uncomfortable conditions, inhabitants are more likely to raise the set temperature. Therefore, when $padj_{SP}$ increases, the heating power consumption in the area will also increase. This trend is easily observable in Figure 17b, where a set point difference of up to 1°C is observed between the minimum and maximum values of $padj_{SP}$. This set point gap due to cold discomfort is therefore maximum for the simulated period (January, coldest month of the year). Simulations made over warmer periods have shown less important set point deviations.

Finally, due to the short duration of the event, the temperature of residential areas usually does not reach its low set value, so the resident rejection is rarely observed. Therefore, in the case of demand-response event of 30 min, the increase of $padj_{SP}$ implies the increase of flexibility potential. In the case of 180 minutes, the lower set point is more likely to be reached, consequently the potential for flexibility was found to decrease with the increase of $padj_{SP}$.

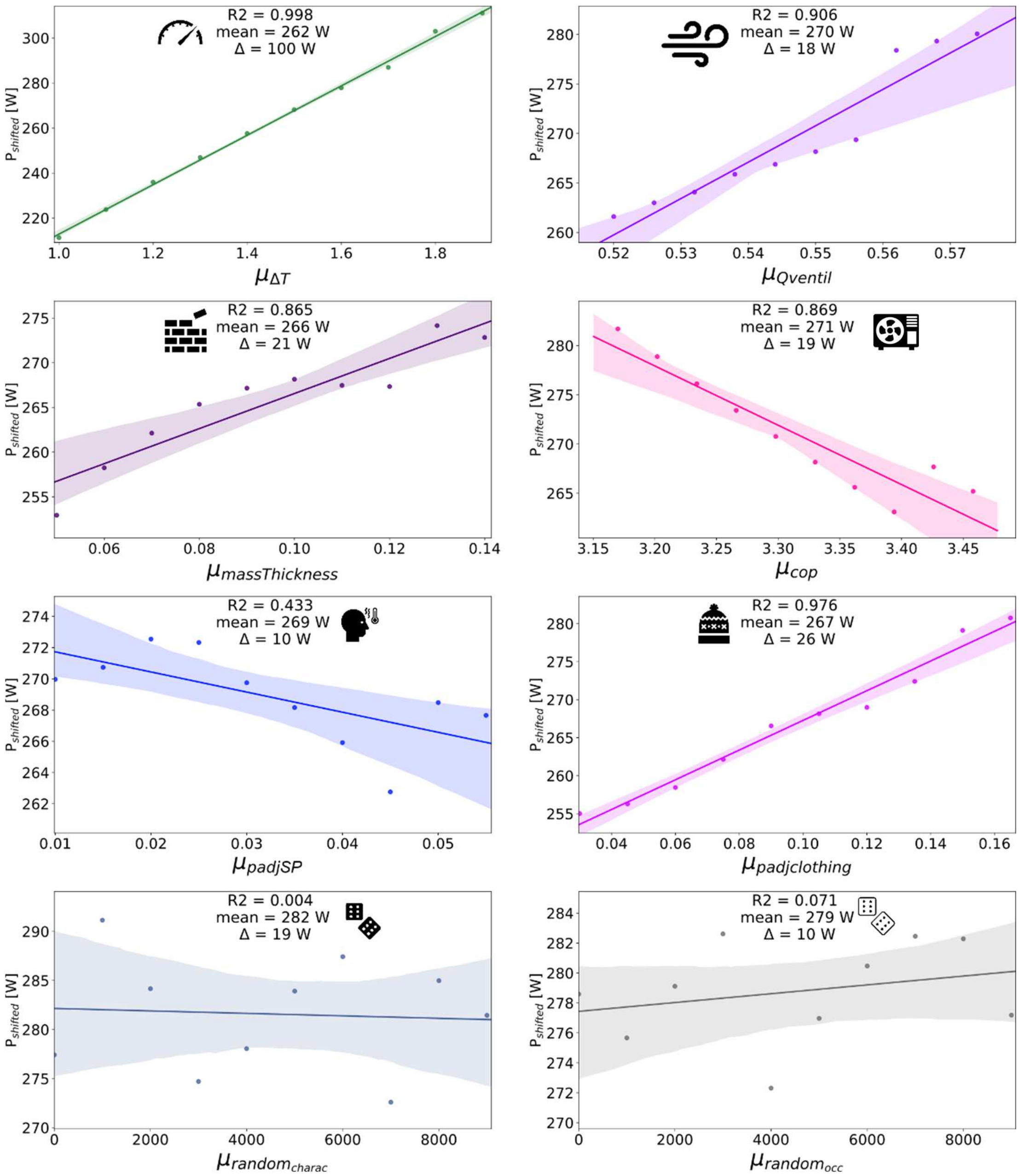

Figure 15 : Regression analysis for the most influential parameters on flexibility potential during the month of January (durationEvent = 180 minutes).

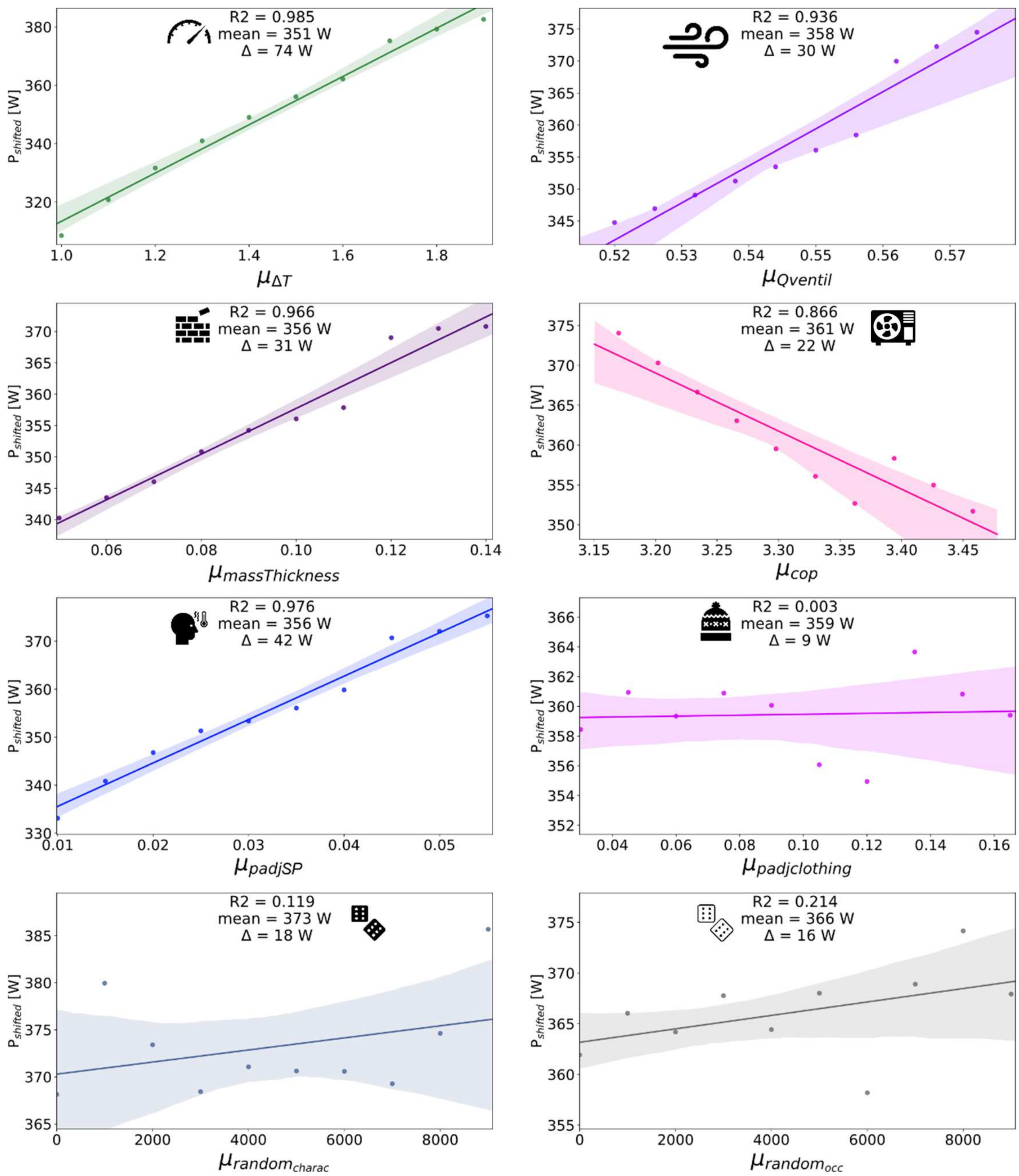

Figure 16 : Regression analysis for the most influential parameters on flexibility potential during the month of January (durationEvent = 30 minutes).

Figure 17 highlights the effect of the adjustment of the clothing insulation and the set point by the occupants on the flexibility potential. Figure 17a shows the variation of the district average heating need, set point and clothes of the neighborhood residents for a single day. The results are presented for the two extreme cases of $padjclothing_{min}$ and $padjclothing_{max}$ adjustments. As expected, the heating consumption is higher when occupants adjust less their clothing to reach their thermal comfort. Indeed, it is found that the set point is higher when the inhabitants adjust less their clothing. Finally, the last graph of Figure 17a enables to observe the dynamics of the adjustment of the clothing over the day, which are mainly due to variations of their activity-related metabolic rate.

Figure 17b presents the same time series but observing this time the effect of the thermostat adjustment parameter. As before, the two extreme cases of thermostat adjustment probabilities are observed: *pajdSP*$_{min}$ and *padjSP*$_{max}$. We observe the effect of the thermostat adjustment by the occupants. During flexibility event, the set point is increased over time in the *padjSP*$_{max}$ case, which reflects the occurrence of flexibility rejection.

Concerning the dynamics of the model outside the DR events, we observe an increase in the set point and heating consumption in the morning, as well as at lunchtime. This is mainly due to the activity of the occupants and their occupancy-related thermostat schedule. Indeed, when waking up, the occupants tend to adjust the set point temperature, as well as at lunchtime when they return home. These trends are observed in Figure 17a and Figure 17b. Concerning the evolution of the clothing coverage, we chose to represent the clothing level only for the active occupants. A decrease in clothing level during the day is observed, due to an increase in both the metabolic rate and the operative temperature.

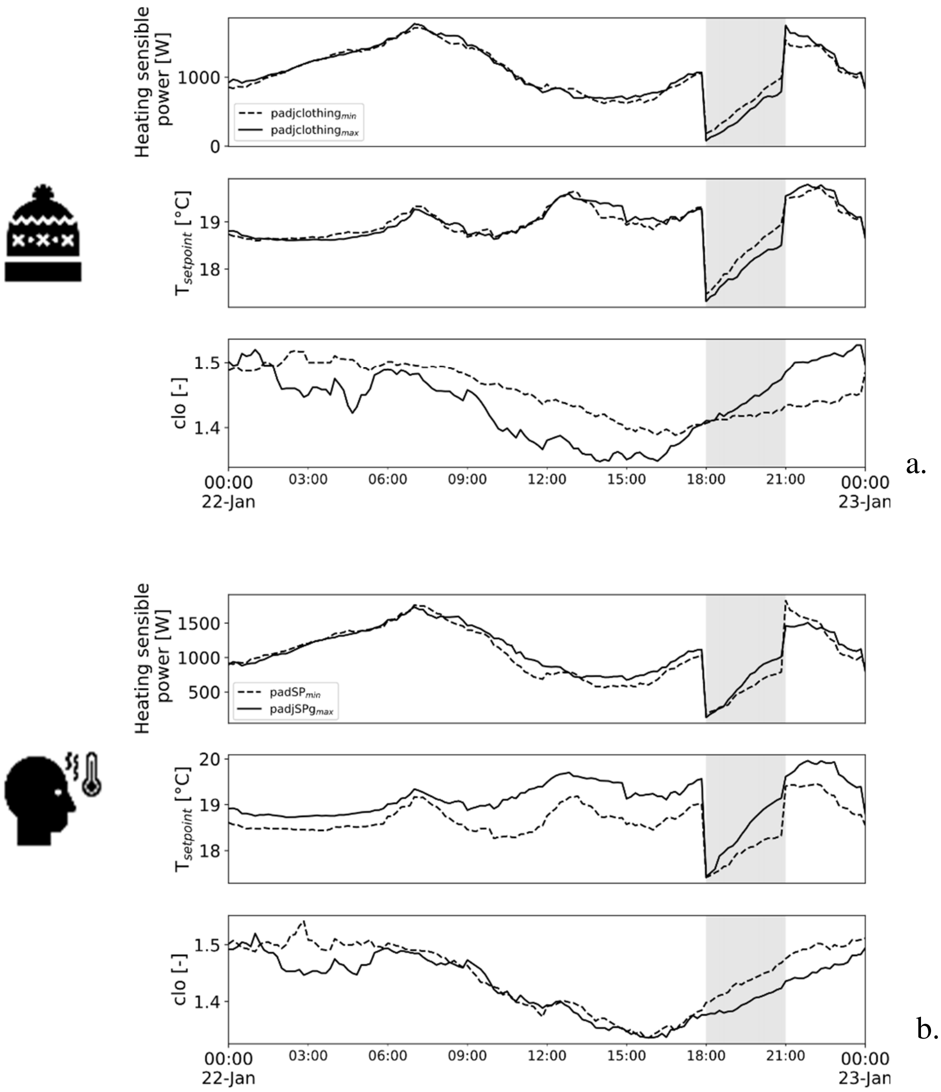

Figure 17 : time series of heating sensible power, set point and clothing level for the 180-min case study ('- -' : minimum value, '—': maximum value)

5.2 Old/new district comparison

The objective of this last study is to evaluate the importance of the building typology on the flexibility. We downgraded the building envelope properties according to the energy audit database (see Annex) giving the median values and standard deviations of U_{wall}, $U_{windows}$, U_{floor} and U_{roof} for buildings constructed during the period 1982-1989 [30]. These average values were set to 0.6, 2.98, 0.4 and 0.33 W/(m²K) respectively. It can be noticed that the standard deviations are larger than for the new district characteristics (Table 2). It should be highlighted that normal distributions might not be the best representation for partly-renovated building fabrics (log-normal distribution could be better suited [59]). However, it was decided to use normal distribution for the sake of repeatability. The heating systems are electric convectors with a thermal efficiency equal to 1, which is representative of French heating systems typical of the 1980s. With respect to the old fabric building characteristics, the average ventilation rate was increased by a factor of 1.6 to account for the higher infiltration rate and the lower ventilation efficiency.

Table 2 : Updated envelope and ventilation properties for the “old” district characteristics

	Name	Description	μ	σ	SA bounds [μ-Δμ; μ+Δμ]	unit
Buildings	Uwall	Heat loss coefficient of the walls	0.6	0.15	[0.57, 0.63]	W/(m²K)
	Uwindow	Heat loss coefficient of the windows	2.98	0.80	[2.81, 3.15]	W/(m²K)
	Ufloor	Heat loss coefficient of the floor	0.4	0.15	[0.37, 0.43]	W/(m²K)
	Uroof	Heat loss coefficient of the roof	0.33	0.1	[0.28, 0.32]	W/(m²K)
	Q_{ventil}	Air change rate	0.8	0.15	[0.85, 0.91]	vol/h

The sensitivity analysis (Figure 18) carried out for the “old” district demonstrates an increase in the flexibility potential compared to the more recent district. Indeed, the average power shifted during January reaches 1292 W, against 290 W found previously. From a general point of view, we observe that the order of the influencing parameter remains the same. Logically, the *cop* parameter disappears for the district with electric convector and the average day set point becomes the 7-th most influential parameter. The overall increase in the μ* parameter can be explained by the decrease in the thermal properties of the buildings. Indeed, the greater the space heating requirements, the greater the potential for flexibility.

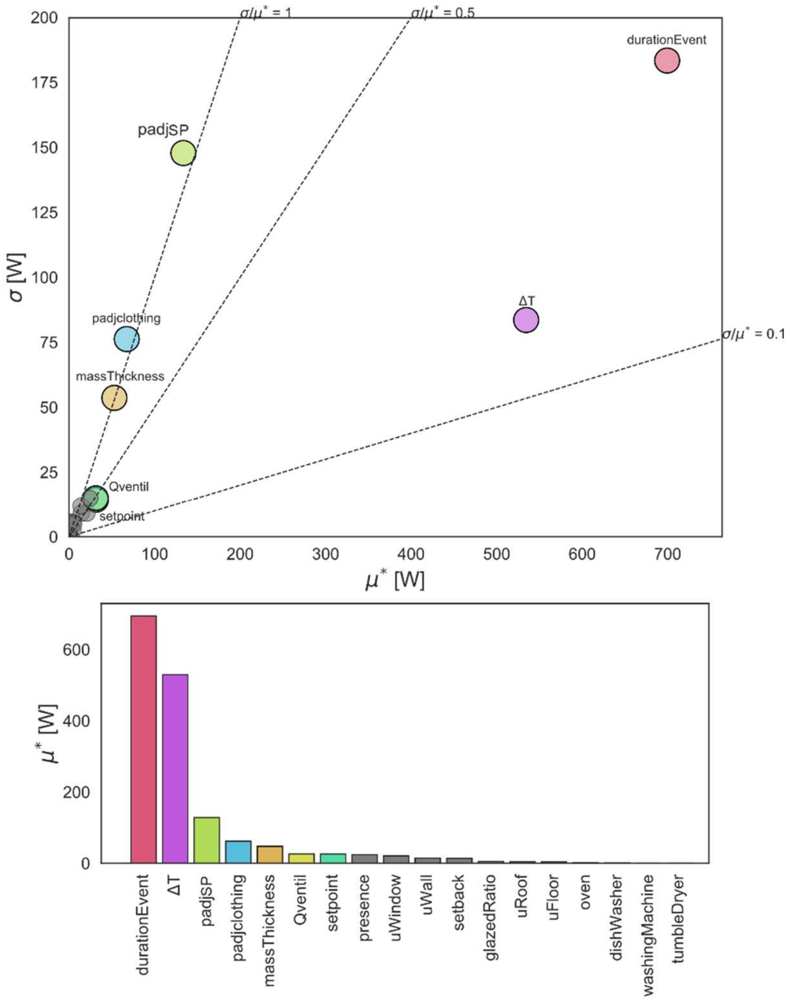

Figure 18 : Sensitivity analysis, σ-μ* plot and μ* distribution for the electric power of the district during the month of January – old fabric district case study – $P_{shifted\ avg}$ = 1292 W

5.3 Discussions

Figure 19 summarizes the results of the uncertainty analysis. For each parameter, the uncertainty is calculated as the range of variation (Δ) divided by the mean value of $P_{shifted}$. For both types of districts, we notice that occupants have a larger influence than the building properties given a district typology. Understanding the way occupants control space heating is thus of main importance to correctly estimate flexibility. This fact indicates the need for further research in occupant behavior. Moreover, it can be observed the relatively higher uncertainty for the old district, due to the larger influence on thermal comfort. This is highlighted by the fact that the set point decrease during the DR event is important for both short and long DR events. On the contrary, short DR events in the new district decrease the influence of occupants' settings.

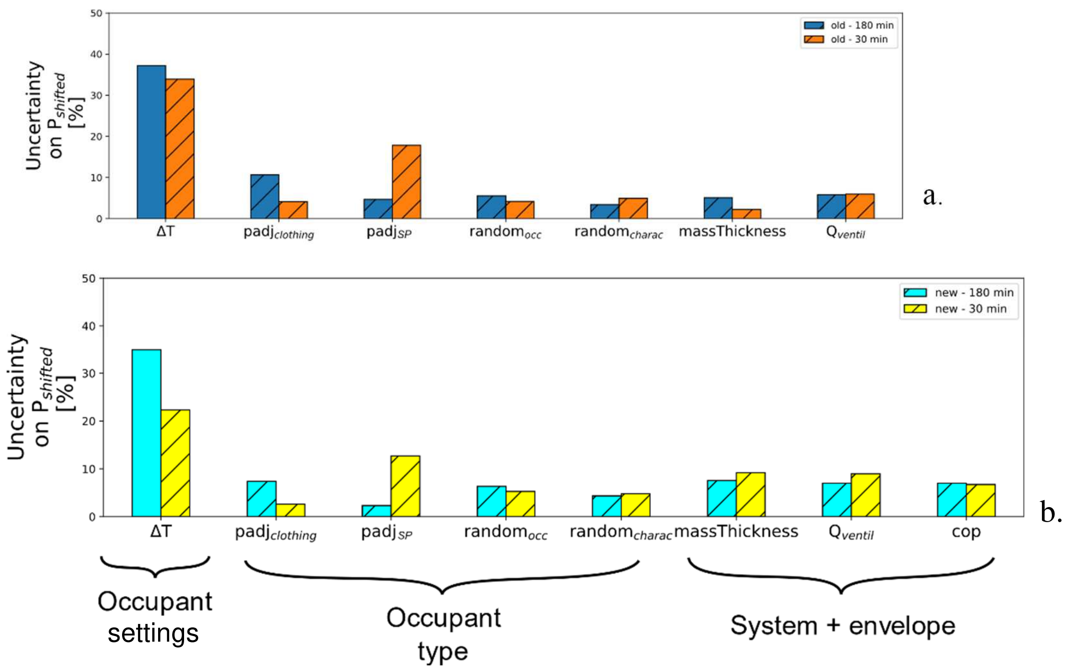

Figure 19 : Relative uncertainty on $P_{shifted}$ for the two district typologies and the two DR event durations.

Despite the broad scope of the study, some limitations should be highlighted. First of all, a district with a different compacity or with more variety of envelopes and systems might alter the conclusions. The relatively good knowledge of input data (from national databases), the homogeneity of systems and the large size of the district favored a strong decrease of some uncertainties. The evaluation of flexibility would be more challenging if some district properties are ill-known (such as construction year or type of heating system). However, this barrier should be overcome with the widespread publication of open-data on building characteristics. Furthermore, the influence of the district size has only been partly addressed in this study. An evaluation for a larger district (674 dwellings, Figure 10) was carried out and led to a slightly lower level of uncertainty.

Regarding the control of the heating system, a thermostat-based flexibility activation and a continuous operation of the heat pumps (*i.e.* variable-speed) were assumed. For a dense residential housing stock, this correctly represents the behavior of the heat pumps. For a single-family house equipped with a heat pump , an on/off working operation of the heat pump should be considered and would affect the availability of flexibility [51]. Changing the time of activation would also influence the flexibility.

Finally, only one type of occupant model was tested. Further investigation should be performed and further data should be collected to challenge the influence of occupants.

6 Conclusions

We have investigated the flexibility potential of a district by estimating its energy consumption from a mono-zone UBEM. Flexibility or DR event were defined as a reduction in the set point from 6 pm, which is classically an overloaded period of the electrical network in winter in France. The occupants, building characteristics and flexibility signal were set in the model according to datasets representing a current French case study. The acceptance of flexibility was modeled by a thermal comfort-based model of occupant thermostat adjustments. Finally, the flexibility potential was defined as the mean shifted power during DR event, and its calculation has been performed for a district of 337 dwellings.

The positive effect of electrical load aggregation was highlighted in the prediction of the electrical load at district level, with a decrease of the uncertainty for groups of more than 50 dwellings. Once the UBEM model was built, a sensitivity analysis and a linear regression analysis were performed to identify the most influential parameters on the results and to better understand the sources of uncertainty on the flexibility potential.

For this winter case study, the space heating represents the greatest potential for flexibility, so we did not consider the flexibility potential on other appliances or systems. The results show the influence of modulation time and set point decrease during demand response event, occupant types and activities. The order of magnitude of the flexibility potential is about 290 W per household for the new district and about 1290 W for the old district. Several key points should be emphasized:

- This study shows the great importance of the duration of the flexibility signal on the results. It appears to be one of the most influential parameters, so it must be carefully selected by the aggregator to optimize the flexibility portfolio.
- Considering DR event duration, it appears that a long-DR events lead to a decrease in the shiftable power. A tradeoff between the power decrease and the duration of activation should thus be defined to optimally activate flexibility.
- Occupants appear to play a key role in flexibility. The dynamic modelling of occupant behavior was carried out and allows the quantification of the occupant rejection phenomenon. The behavior of occupants must be carefully taken into account when estimating the flexibility potential.
- Finally, the characteristics of the buildings did not show a too large uncertainty in the resulting flexibility at district level. Indeed, the aggregation effect was sufficient enough to dampen the diversity observed in the building databases. This conclusion is valid only if the construction period and the heating system are roughly known.

This work paves the way of the flexibility characterization at district level by quantifying the source of uncertainties using a UBEM model. In future work, a focus on the most influencing parameter can be done, while considering fewer other parameters with less influence, which can improve the efficiency of the characterization of flexibility. Moreover, the strong influence of climate and flexibility signal underlines the future need for “smart” controllers in buildings.

7 Acknowledgements

This research was funded by the French National Research Agency, CLEF project (ANR-17-CE22-0005-01).

Annex: Summary of the used datasets

Category	Name	Type	Geographical area	Year of data collection	Size	Ref.
National grid	RTE (residual load)	Database	France	2017	-	[60]
Geometry	BDTOPO (land register)	Database	France	2020	-	[61]
Buildings	DPE (energy audit of existing buildings)	Database	Department (Charente-Maritime, 17)	2013-2020	71 000 households, 1831 of similar type	[62]
	RT 2012 (new building regulation)	Database	Metropolitan France	2012-2020	136 811 households	[55]
	OQAI survey (ventilation rates)	Survey	Metropolitan France	2003–2005	567 households	[33]
Occupants	Population census (household composition et taux d'équipement)	Survey	Metropolitan France	2010-2015	28 million households	[64]
	Time Use Survey (activities)	Survey	Metropolitan France	2009-2010	13 950 individuals from 12 000 households	[65]
	EcoBee (smart thermostats)	Appliance Monitoring	Canada	2015-2020	9 000 households	[43]
	PHEBUS survey (heating habits and applicances ownership)	Survey	Metropolitan France	2013	5 345 households	[66]
	PEDOBUR and EQL'ORE projects (usage based on ToU)	Survey	La Rochelle, France	2019	99 households	x
	LINEAR project (shifting probabilities)	Appliance Monitoring	Flanders region, Belgium	2009-2014	186 households	[67]
Appliances	EU energy labelling of appliances (energy efficiency)	Regulation	Europe		-	[68]
	TOPTEN-Ademe (energy class and size)	Market data	France	2004-2014	90% of market	[69]
	REMODECE project (energy class and size)	Appliance Monitoring	Auvergne-Rhône-Alpes region, France	2008	103 households	[70]
	FROIDLAVAGE monitoring campaign (usage)	Appliance Monitoring	Metropolitan France	2015-2016	107 households	[71]
	ADEME survey campaign (usage)	Survey	Metropolitan France	2015	1 001 households	[72]

References

[1] P.D. Lund, J. Lindgren, J. Mikkola, J. Salpakari, Review of energy system flexibility measures to enable high levels of variable renewable electricity, Renewable and Sustainable Energy Reviews. 45 (2015) 785–807. https://doi.org/10.1016/j.rser.2015.01.057.

[2] World Business Council for Sustainable Development, Transforming the Market, 2009. https://www.wbcsd.org/Programs/Cities-and-Mobility/Resources/Transforming-the-Market-Energy-Efficiency-in-Buildings.

[3] IEA, IEA report, Chap. 6 Buildings sector energy consumption, (2016). https://www.eia.gov/outlooks/ieo/pdf/buildings.pdf (accessed September 25, 2020).

[4] K.M. Luc, R. Li, L. Xu, T.R. Nielsen, J.L.M. Hensen, Energy flexibility potential of a small district connected to a district heating system, Energy and Buildings. 225 (2020) 110074. https://doi.org/10.1016/j.enbuild.2020.110074.

[5] S.Ø. Jensen, A. Marszal-Pomianowska, R. Lollini, W. Pasut, A. Knotzer, P. Engelmann, A. Stafford, G. Reynders, IEA EBC Annex 67 Energy Flexible Buildings, Energy and Buildings. 155 (2017) 25–34. https://doi.org/10.1016/j.enbuild.2017.08.044.

[6] H. Johra, P. Heiselberg, J. Le Dréau, Influence of envelope, structural thermal mass and indoor content on the building heating energy flexibility, Energy and Buildings. 183 (2019) 325–339. https://doi.org/10.1016/j.enbuild.2018.11.012.

[7] M. Hu, F. Xiao, Quantifying uncertainty in the aggregate energy flexibility of high-rise residential building clusters considering stochastic occupancy and occupant behavior, Energy. 194 (2020) 116838. https://doi.org/10.1016/j.energy.2019.116838.

[8] J. Dickert, P. Schegner, Residential Load Models for Network Planning Purposes, (n.d.) 7.

[9] I.D. Jaeger, G. Reynders, D. Saelens, T. Park, Quantifying Uncertainty Propagation For The District Energy Demand Using Realistic Variations On Input Data, in: 2019. https://doi.org/10.26868/25222708.2019.210923.

[10] J. Sala, R. Li, M.H. Christensen, Clustering and classification of energy meter data: A comparison analysis of data from individual homes and the aggregated data from multiple homes, Build. Simul. 14 (2021) 103–117. https://doi.org/10.1007/s12273-019-0587-4.

[11] Y.Q. Ang, Z.M. Berzolla, C.F. Reinhart, From concept to application: A review of use cases in urban building energy modeling, Applied Energy. 279 (2020) 115738. https://doi.org/10.1016/j.apenergy.2020.115738.

[12] M. Ferrando, F. Causone, T. Hong, Y. Chen, Urban building energy modeling (UBEM) tools: A state-of-the-art review of bottom-up physics-based approaches, Sustainable Cities and Society. 62 (2020) 102408. https://doi.org/10.1016/j.scs.2020.102408.

[13] F. Johari, G. Peronato, P. Sadeghian, X. Zhao, J. Widén, Urban building energy modeling: State of the art and future prospects, Renewable and Sustainable Energy Reviews. 128 (2020) 109902. https://doi.org/10.1016/j.rser.2020.109902.

[14] C.F. Reinhart, C. Cerezo Davila, Urban building energy modeling – A review of a nascent field, Building and Environment. 97 (2016) 196–202. https://doi.org/10.1016/j.buildenv.2015.12.001.

[15] I. De Jaeger, J. Lago, D. Saelens, A probabilistic building characterization method for district energy simulations, Energy and Buildings. 230 (2021) 110566. https://doi.org/10.1016/j.enbuild.2020.110566.

[16] D.V. Likhachev, Parametric sensitivity analysis as an essential ingredient of spectroscopic ellipsometry data modeling: An application of the Morris screening method, Journal of Applied Physics. 126 (2019) 184901. https://doi.org/10.1063/1.5126074.

[17] J. Vivian, U. Chiodarelli, G. Emmi, A. Zarrella, A sensitivity analysis on the heating and cooling energy flexibility of residential buildings, Sustainable Cities and Society. 52 (2020) 101815. https://doi.org/10.1016/j.scs.2019.101815.

[18] Z. Ma, A. Knotzer, J.D. Billanes, B.N. Jørgensen, A literature review of energy flexibility in district heating with a survey of the stakeholders' participation, Renewable and Sustainable Energy Reviews. 123 (2020) 109750. https://doi.org/10.1016/j.rser.2020.109750.

[19] F. Scarpa, L.A. Tagliafico, V. Bianco, Financial and energy performance analysis of efficiency measures in residential buildings. A probabilistic approach, Energy. 236 (2021) 121491. https://doi.org/10.1016/j.energy.2021.121491.

[20] V. Masson, J. Hidalgo, A. Amossé, F. Belaid, E. Bocher, M. Bonhomme, A. Bourgeois, G. Bretagne, S. Caillerez, E. Cordeau, C. Demazeux, S. Faraut, C. Gallato, S. Haouès-Jouve, M.-L. Lambert, A. Lemonsu, R. Lestringant, J.-P. Levy, N. Long, C.X. Lopez, M. Pellegrino, G. Petit, C. Pignon-Mussaud, C. Plumejeaud-Perreau, V. Ruff, R. Schoetter, N. Tornay, D.D. Vye, Urban Climate, Human behavior & Energy consumption: from LCZ mapping to simulation and urban planning (the MapUCE project), in: 9th International Conference on Urban Climate, CNRM - Météo France, Toulouse, France, 2015. https://hal.archives-ouvertes.fr/hal-01252761 (accessed September 28, 2020).

[21] M. Vellei, S. Martinez, J. Le Dréau, Agent-based stochastic model of thermostat adjustments: A demand response application, Energy and Buildings. 238 (2021) 110846. https://doi.org/10.1016/j.enbuild.2021.110846.

[22] Smart Thermostats & Smart Home Devices | ecobee, (n.d.). https://www.ecobee.com/en-us/ (accessed March 17, 2021).

[23] P. Riederer, V. Partenay, N. Perez, C. Nocito, R. Trigance, T. Guiot, Development of a simulation platform for the evaluation of district energy system performances, (2015). https://doi.org/10.13140/RG.2.1.4668.8401/1.

[24] N. Perez, P. Riederer, C. Inard, V. Partenay, Thermal building modelling adapted to district energy simulation, (2015). https://doi.org/10.13140/RG.2.1.3714.2163/1.

[25] E. Garreau, Y. Abdelouadoud, E. Herrera, W. Keilholz, G.-E. Kyriakodis, V. Partenay, P. Riederer, District MOdeller and SIMulator (DIMOSIM) – A dynamic simulation platform based on a bottom-up approach for district and territory energetic assessment, Energy and Buildings. 251 (2021) 111354. https://doi.org/10.1016/j.enbuild.2021.111354.

[26] L. Frayssinet, Adapting buildings heating and cooling power need models at the district scale, (n.d.) 253.

[27] J. Sokol, C. Cerezo Davila, C.F. Reinhart, Validation of a Bayesian-based method for defining residential archetypes in urban building energy models, Energy and Buildings. 134 (2017) 11–24. https://doi.org/10.1016/j.enbuild.2016.10.050.

[28] seaborn.distplot — seaborn 0.11.2 documentation, (n.d.). https://seaborn.pydata.org/generated/seaborn.distplot.html (accessed September 6, 2021).

[29] M. Shin, J.S. Haberl, Thermal zoning for building HVAC design and energy simulation: A literature review, Energy and Buildings. 203 (2019) 109429. https://doi.org/10.1016/j.enbuild.2019.109429.

[30] Observatoire des performances énergétiques (OPE) - data.gouv.fr, (n.d.). https://www.data.gouv.fr/fr/datasets/observatoire-des-performances-energetiques/ (accessed September 23, 2020).
[31] Diagnostics de performance énergétique pour les logements par habitation - data.gouv.fr, (n.d.). /fr/datasets/diagnostics-de-performance-energetique-pour-les-logements-par-habitation/ (accessed January 15, 2021).
[32] O. Ruhnau, L. Hirth, A. Praktiknjo, Time series of heat demand and heat pump efficiency for energy system modeling, Sci Data. 6 (2019) 189. https://doi.org/10.1038/s41597-019-0199-y.
[33] S. Langer, O. Ramalho, M. Derbez, J. Ribéron, S. Kirchner, C. Mandin, Indoor environmental quality in French dwellings and building characteristics, Atmospheric Environment. 128 (2016) 82–91. https://doi.org/10.1016/j.atmosenv.2015.12.060.
[34] M. Vellei, J. Le Dréau, S.Y. Abdelouadoud, Predicting the demand flexibility of wet appliances at national level: The case of France, Energy and Buildings. 214 (2020) 109900. https://doi.org/10.1016/j.enbuild.2020.109900.
[35] M. Vellei, J.L. Dréau, On the prediction of dynamic thermal comfort under uniform environments, in: 2020: p. 424. https://hal-univ-rochelle.archives-ouvertes.fr/hal-02556047 (accessed March 17, 2021).
[36] M. Vellei, S. Martinez, J. Le Dréau, Agent-based stochastic model of thermostat adjustments: a demand response application, Energy and Buildings. (2021) 110846. https://doi.org/10.1016/j.enbuild.2021.110846.
[37] Statistical presentation − Statistics on income and living conditions 2010 | Insee, (n.d.). https://www.insee.fr/en/metadonnees/source/operation/s1074/presentation (accessed January 15, 2021).
[38] Statistical presentation − Time use survey 2009-2010 | Insee, (n.d.). https://www.insee.fr/en/metadonnees/source/operation/s1362/presentation (accessed November 17, 2020).
[39] B.F. Balvedi, E. Ghisi, R. Lamberts, A review of occupant behaviour in residential buildings, Energy and Buildings. 174 (2018) 495–505. https://doi.org/10.1016/j.enbuild.2018.06.049.
[40] ANSI/ASHRAE Addendum g to ANSI/ASHRAE Standard 55-2010, (n.d.) 8.
[41] Enquête Performance de l'Habitat, Équipements, Besoins et Usages de l'énergie (Phébus) | Données et études statistiques, (n.d.). https://www.statistiques.developpement-durable.gouv.fr/enquete-performance-de-lhabitat-equipements-besoins-et-usages-de-lenergie-phebus (accessed January 15, 2021).
[42] Ademe, Projet PECOIC - Prise en compte du comportement des occupants et incertitudes associées en phase conception de bâtiments, 2019.
[43] Donate your Data Smart Wi-Fi Thermostats by ecobee, (n.d.). https://www.ecobee.com/donate-your-data/ (accessed November 17, 2020).
[44] M. Humphreys, F. Nicol, S. Roaf, Adaptive Thermal Comfort: Foundations and Analysis, Taylor & Francis Group, London, 2015.
[45] A.S. Rao, M.P. Georgeff, BDI Agents: From Theory to Practice, in: ICMAS95: 1st INTERNATIONAL CONFERENCE ON MULTI-AGENT SYSTEMS, San Francisco (USA), 1995. https://doi.org/10.1.1.37.7970.
[46] F. Tartarini, S. Schiavon, T. Cheung, T. Hoyt, CBE Thermal Comfort Tool: Online tool for thermal comfort calculations and visualizations, SoftwareX. 12 (2020) 100563. https://doi.org/10.1016/j.softx.2020.100563.

[47] BESTEST-EX: Building Energy Simulation Test for Existing Homes, (n.d.). https://www.nrel.gov/buildings/bestest-ex.html (accessed February 18, 2021).
[48] D. Saelens, I. De Jaeger, F. Bünning, M. Mans, A. Maccarini, E. Garreau, Ø. Rønneseth, I. Sartori, A. Vandermeulen, B. van der Heijde, L. Helsen, Towards a DESTEST: a District Energy Simulation Test Developed in IBPSA Project 1, 2019. https://doi.org/10.26868/25222708.2019.210806.
[49] É. Vorger, Étude de l'influence du comportement des habitants sur la performance énergétique du bâtiment, phdthesis, Ecole Nationale Supérieure des Mines de Paris, 2014. https://pastel.archives-ouvertes.fr/tel-01144461 (accessed November 19, 2020).
[50] Å.L. Sørensen, I. Sartori, K.B. Lindberg, I. Andresen, Electricity analysis for energy management in neighbourhoods: Case study of a large housing cooperative in Norway, 1343. (2019). https://ntnuopen.ntnu.no/ntnu-xmlui/handle/11250/2629829 (accessed November 19, 2020).
[51] D. Fischer, T. Wolf, J. Wapler, R. Hollinger, H. Madani, Model-based flexibility assessment of a residential heat pump pool, Energy. 118 (2017) 853–864. https://doi.org/10.1016/j.energy.2016.10.111.
[52] European smart grids task force, Final report: demand side flexibility, perceived barriers and proposed recommendations, 2019. https://ec.europa.eu/energy/sites/ener/files/documents/eg3_final_report_demand_side_flexiblity_2019.04.15.pdf (accessed February 10, 2021).
[53] A. Wang, R. Li, S. You, Development of a data driven approach to explore the energy flexibility potential of building clusters, Applied Energy. 232 (2018) 89–100. https://doi.org/10.1016/j.apenergy.2018.09.187.
[54] M.D. Morris, Factorial Sampling Plans for Preliminary Computational Experiments, Technometrics. 33 (1991) 161–174. https://doi.org/10.2307/1269043.
[55] E. Borgonovo, E. Plischke, Sensitivity analysis: A review of recent advances, European Journal of Operational Research. 248 (2016) 869–887. https://doi.org/10.1016/j.ejor.2015.06.032.
[56] B. Iooss, P. Lemaître, A Review on Global Sensitivity Analysis Methods, in: G. Dellino, C. Meloni (Eds.), Uncertainty Management in Simulation-Optimization of Complex Systems: Algorithms and Applications, Springer US, Boston, MA, 2015: pp. 101–122. https://doi.org/10.1007/978-1-4899-7547-8_5.
[57] J.D. Herman, J.B. Kollat, P.M. Reed, T. Wagener, Technical note: Method of Morris effectively reduces the computational demands of global sensitivity analysis for distributed watershed models, Hydrol. Earth Syst. Sci. Discuss. 10 (2013) 4275–4299. https://doi.org/10.5194/hessd-10-4275-2013.
[58] W. Tian, Y. Heo, P. de Wilde, Z. Li, D. Yan, C.S. Park, X. Feng, G. Augenbroe, A review of uncertainty analysis in building energy assessment, Renewable and Sustainable Energy Reviews. 93 (2018) 285–301. https://doi.org/10.1016/j.rser.2018.05.029.
[59] G. Petrou, A. Mavrogianni, P. Symonds, M. Davies, Beyond Normal: Guidelines on How to Identify Suitable Model Input Distributions for Building Performance Analysis, (n.d.) 8.
[60] Schedule of Tempo-type supply offerings - RTE Services Portal, Portail Services RTE. (n.d.). https://www.services-rte.com/en/view-data-published-by-rte/schedule-of-Tempo-type-supply-offerings.html (accessed March 12, 2021).

[61] Géoservices | Accéder au téléchargement des données libres IGN, (n.d.). https://geoservices.ign.fr/documentation/diffusion/telechargement-donnees-libres.html (accessed March 12, 2021).

[62] ADEME, Diagnostics de performance énergétique pour les logements par habitation, (2020). https://data.ademe.fr/datasets/dpe-france (accessed March 17, 2021).

[63] Observatoire des performances énergétiques (OPE) - data.gouv.fr, (n.d.). /fr/datasets/observatoire-des-performances-energetiques/ (accessed March 18, 2021).

[64] INSEE, 2015 Population census, (2015). https://www.insee.fr/en/metadonnees/source/serie/s1321.

[65] INSEE, 2009-2010 Time Use Survey, (2010). https://www.insee.fr/en/metadonnees/source/operation/s1362/presentation.

[66] SDES, PHEBUS CLODE: Enquête Performance de l'Habitat, Equipements, Besoins et USages de l'énergie - volet CLODE, 2013.

[67] R. D'hulst, W. Labeeuw, B. Beusen, S. Claessens, G. Deconinck, K. Vanthournout, Demand response flexibility and flexibility potential of residential smart appliances: Experiences from large pilot test in Belgium, Applied Energy. 155 (2015) 79–90. https://doi.org/10.1016/j.apenergy.2015.05.101.

[68] Commission Delegated Regulation (EU) No 392/2012 of 1 March 2012 supplementing Directive 2010/30/EU of the European Parliament and of the Council with regard to energy labelling of household tumble driersText with EEA relevance, (n.d.) 26.

[69] Energy efficiency of White Goods in Europe: monitoring the market with sales ..., ADEME. (n.d.). https://www.ademe.fr/energy-efficiency-of-white-goods-in-europe-monitoring-the-market-with-sales-data-0 (accessed March 17, 2021).

[70] A. de Almeida, P. Fonseca, B. Schlomann, N. Feilberg, C. Ferreira, Residential Monitoring to Decrease Energy Use and Carbon Emissions in Europe (REMODECE), 2008.

[71] Campagne de mesures des appareils de production de froid, des appareils de lavage et de la climatisation, (2016) 179.

[72] Etude Usage Lavage Domestique, ADEME. (n.d.). https://www.ademe.fr/etude-usage-lavage-domestique (accessed March 18, 2021).